NAVY DEPARTMENT
THE DAVID W. TAYLOR MODEL BASIN
WASHINGTON 7, D.C.

A THEORETICAL AND EXPERIMENTAL INVESTIGATION OF A DYNAMICALLY LOADED RING WITH RADIAL ELASTIC SUPPORT

by

Edward Wenk, Jr., Dr. Eng.

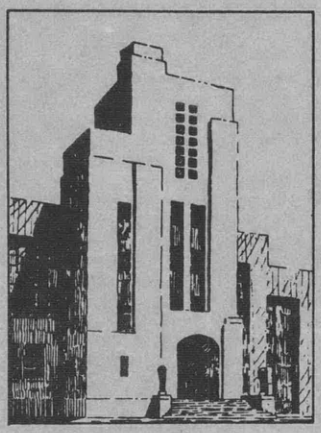

July 1950

Report 704

NS 870-001

INITIAL DISTRIBUTION

Copies

14 Chief, BuShips, Project Records (Code 362), for distribution:
- 5 Project Records
- 1 Technical Assistant (Code 106)
- 1 Research (Code 330)
- 1 Applied Science (Code 370)
- 1 Preliminary Design (Code 421)
- 1 Underwater Explosion Research (Code 423)
- 1 Hull Design (Code 440)
- 1 Hull Design, Scientific (Code 442)
- 1 Submarines (Code 515)
- 1 Minesweeping (Code 620)

2 Commander, Naval Ordnance Laboratory, Explosives Division, White Oak, Silver Spring, Maryland

2 Chief, Office of Naval Research, Mechanics and Materials Branch, Washington, D.C.

2 Commander, Norfolk Naval Shipyard, Underwater Explosions Research Unit, Code 205, Portsmouth, Virginia

2 Commander, Portsmouth Naval Shipyard, Portsmouth, New Hampshire

1 Commander, Naval Ordnance Test Station, Inyokern, China Lake, Calif.

2 Director, Naval Research Laboratory, Washington 20, D.C.

1 Manager, U.S. Naval Aircraft Factory, NAMC, Philadelphia 12, Pa.

1 CO, U.S. Naval Air Missile Test Center, Point Mugu, California In care of U.S. Naval Station, Port Hueneme, Calif.

1 Director, Naval Engineering Experiment Station, Annapolis, Md.

1 Director, U.S. Navy Electronics Laboratory, San Diego 52, California.

1 Superintendent, U.S. Naval Gun Factory, Washington 25, D.C.

1 Commander, Naval Proving Ground, Dahlgren, Va.

1 Commander, New York Naval Shipyard, Naval Base Station, Brooklyn 1, N.Y.

1 Commander, Operational Development Force, U.S. Naval Base, Norfolk 11, Virginia.

1 Director, Office of Naval Intelligence (Op-322-F2) Washington, D.C.

1 Officer-in-Charge, Naval Ordnance Development Unit, Applied Physics Lab., Johns Hopkins University, 8621 Georgia Avenue, Silver Spring, Maryland.

Copies

1 Chief of Naval Operations, Operations Evaluation Group, Op34H8, Navy Department, Washington 25, D.C.

1 Chief, Bureau of Yards and Docks, Navy Department, Washington 25, D.C.

1 Chief, Bureau of Ordnance, Navy Department, Washington 25, D.C. Attn: Ad-3, Technical Library, Re9a

1 Chief, Bureau of Aeronautics, Navy Department, Washington 25, D.C. TD-41, Technical Library, DE-22, C.W. Hurley

3 Commander, Naval Ordnance Laboratory, White Oak, Silver Spring, Md., Attn: Dr. C A. Truesdell, Messrs. J.L. New and W. Mostow

1 Director, Naval Air Experimental Station, Naval Air Material Center, Naval Base, Philadelphia 12, Pa.

1 Under Secretary of Navy Assistant, Research and Development, Washington, D.C.

1 Superintendent, Post Graduate School, U.S. Naval Academy, Annapolis, Md.

1 Commanding Officer, U.S. Navy Material Laboratory, Naval Base Station, Brooklyn 1, N.Y.

1 U.S. Coast Guard, 1300 E Street, N.W. Washington, D.C. Attn: Chief, Testing and Development Division

1 Research and Development Board, The Pentagon, Washington 25, D.C. Attn: Library, Code 3D641

1 Director, Technical Information Branch, U.S. Army Proving Ground, Aberdeen, Md.

1 Commanding General, U.S. Air Forces, The Pentagon, Washington 25, D.C. Attn: Research and Development Division

1 Commanding General, Air Materiel Command, Wright-Patterson Air Force Base, Dayton, Ohio. Attn: E.H. Schwartz (MCREXA-8)

1 Office of Chief of Ordnance, Research and Development Service, Department of the Army, The Pentagon, Washington 25, D.C. Attn: ORDTB

1 Commanding Officer, Engineer Board, Ft. Belvoir, Va.

1 Chief of Staff, Department of the Army, The Pentagon, Washington 25, D.C. Attn: Director of Research and Development

5 Director of Aeronautical Research, NACA, 1724 F St., N.W. Washington, D.C.

1 U.S. Atomic Energy Commission, Division of Research, Washington, D.C.

2 Director, National Bureau of Standards, Washington, D.C. Attn: Dr. W.H. Ramberg

Copies

1 Head, Department of Naval Architecture and Marine Engineering, Massachusetts Institute of Technology, Cambridge, Mass.

1 Director, Institute for Mathematics and Mechanics, New York University, 45 Fourth Avenue, New York 3, N.Y.

1 Armour Research Foundation, 35 W. 33rd Street, Chicago 16, Ill.

1 Franklin Institute of the State of Pennsylvania, Parkway at Twentieth Street, Philadelphia 3, Penna.

1 Electric Boat Company, Groton, Conn.

1 Dr. S.P. Timoshenko, School of Engineering, Stanford University, Stanford, Calif.

1 Dr. W. Prager, Graduate Division of Applied Mathematics, Brown University, Providence, R.I.

1 Dr. N.J. Hoff, Department of Aeronautical Engineering and Applied Mechanics, Polytechnic Institute of Brooklyn, 99 Livingston St., Brooklyn, N.Y.

1 Dr. N.M. Newmark, Department of Civil Engineering, University of Illinois, Urbana, Ill.

1 Dr. J.N. Goodier, School of Engineering, Stanford University, Stanford, Calif.

1 Prof. F.K Teichmann, Department of Aeronautical Engineering, New York University, University Heights, New York, N.Y.

1 Prof. L S. Jacobsen, Stanford University, Stanford, Calif.

1 Prof. Jesse Ormondroyd, University of Michigan, Ann Arbor, Mich.

1 Dr. W H. Hoppmann, Mechanical Engineering Department, The Johns Hopkins University, Baltimore, Md.

1 Prof. R.M Hermes, University of Santa Clara, Santa Clara, Calif.

1 Prof. E. Reissner, Department of Mathematics, Massachusetts Institute of Technology, Cambridge, Mass.

1 Prof. L H. Donnell, Illinois Institute of Technology, Technology Center, Chicago 16, Ill.

1 Dr. J.M. Lessells, Journal of Applied Mechanics, Massachusetts Institute of Technology, Cambridge 39, Mass.

1 Dr. W R. Osgood, Armour Research Foundation, 221 E. Cullerton St., Chicago 16, Ill.

1 Prof. H.M. Westergaard, Harvard University, Cambridge, Mass.

NOTATION

A	Area of cross section of ring
a_i	Generalized coordinates
B	Normal force on cross section of ring
b	Width of spring
C, D	Constants
d	Stroke of the pendulum
E	Modulus of elasticity
E_i, F_i	Constants
f	Natural frequency of leaf spring
g	Acceleration of gravity
h	Thickness of leaf spring
I	Moment of inertia of cross section of ring about x-x axis
i	An integer designating the mode of vibration
K	Lumped constant for springs of constant k_n which simulate elastic foundation
k_n	Stiffness constant for individual springs which simulate elastic foundation
k	Modulus of elastic foundation, radial
L	Length of pendulum
l	Length of leaf spring
M	Flexural couple acting on cross section of ring about x-x axis, taken positive if it increases the curvature of the ring
m	Modulus of elastic foundation, tangential
N	Shear on cross section of ring in a radial direction
P	External load, force per inch circumference, positive toward center
P_o	Maximum value of P
p_i	Circular frequency of vibrating ring at mode i
Q_i	Generalized external force, positive toward center
q_{cr}	Static buckling load on ring
r	Radius of ring
s	Circumference of ring
T	Kinetic energy
t	Time variable
t_1	Specific time at which behavior is stated
U	Radial displacement function
u	Radial displacement of ring, measured positive toward center

V	Potential energy
$\bar{v}$	Terminal velocity of body at time of impact with ring
W	Tangential displacement function
W_r	Lumped weight of ring and spring system
W_p	Weight of body striking ring
w	Tangential displacement of ring, measured positive if counterclockwise
α, β	Constants
Γ	Time function
γ	Density
Δ	Deflection of leaf spring
η_i	ω_i / p_i
θ	Central angle of ring, measured positive counterclockwise
ν, μ	Constants
σ	Bending stress in leaf spring
τ	Duration of half-sine pulse
ω	Circular frequency of external periodic exciting force, $\omega = \pi/\tau$

TABLE OF CONTENTS

	Page
ABSTRACT	1
1. INTRODUCTION	1
2. THEORETICAL ANALYSIS	3
A. Statement of the Problem	3
B. The Differential Equation of Motion	4
C. Frequency Equation for Free Vibration of Elastically Supported Ring	6
D. Radial Displacements and Bending Moments Caused by a Concentrated Harmonic Force	7
E. Radial Displacements and Bending Moments with Transient Loading	10
F. Static Loading Treated as Limiting Case of Transient Loading	12
G. Discussion of Solution in Series Form	12
H. Comparison of Series Solution with a Closed-Form Solution for the Case of Static Load	13
I. Numerical Example of Series Solution with Dynamic Loading	15
J. Discussion of Response Pattern During and After Application of Load	17
3. EXPERIMENTAL ANALYSIS	22
A. Statement of Objectives	23
B. Planning of Experiment	23
C. Description of the Ring and Elastic Support	23
D. Pulse Generator for Applying Transient Loads	24
E. The Load Dynamometer	26
F. Excitation of Steady-State Forced Vibrations	28
G. Instrumentation to Measure Strain and Displacement	28
H. Recording Equipment	29
4. EXPERIMENTAL RESULTS AND COMPARISON WITH THEORY	29
A. Test Procedures	31
B. Results of Steady-State Vibration Tests	31
C. Comparison of Observed and Computed Frequencies of Free Vibration	31
D. Discussion of Rigid-Body Translation and the Presence of Tangential Constraint	32
E. Tests with Transient Load	34
F. Comparison Between Observed and Theoretical Strains and Displacements	37

Page

G. Discussion of Linear Response with Respect to Intensity of Load 38

H. Discussion of Agreement Between Observed and Theoretical Response for Transient Load 41

I. Discussion of Range of Parameters Explored Experimentally . . 41

5. SUMMARY AND CONCLUSIONS 42

A. Restatement of Important Equations of Response 42

B. Experimental Investigation 42

C. Agreement Between Theory and Experiment 43

D. Conclusions 43

ACKNOWLEDGMENT 43

APPENDIX 1 - APPLICATIONS 44

A. Graphical Solution of Frequency Equation 44

B. Strength Calculation of Rings 44

C. Possible Limitations of Theory Due to Simplifying Assumptions 46

APPENDIX 2 - DETAILS OF EXPERIMENTAL APPARATUS AND TEST INSTRUMENTATION 46

A. Introduction 46

B. Description of the Ring 46

C. Description of Elastic Support 47

D. Design of Pulse Generator for Applying Transient Loads . . . 52

1. Guided Ballistic Pendulum 53

2. Design of Pendulum as Pulse Generator 54

E. The Load Dynamometer 56

F. Excitation of Steady-State Forced Vibrations 61

G. Instrumentation to Measure Strain and Displacements 62

H. Auxiliary Amplifying and Recording Equipment 64

I. Discussion of Experimental Errors 66

REFERENCES 68

BIBLIOGRAPHY 70

A THEORETICAL AND EXPERIMENTAL INVESTIGATION OF A DYNAMICALLY LOADED RING WITH RADIAL ELASTIC SUPPORT

by

Edward Wenk, Jr., Dr. Eng.

ABSTRACT

The study of free vibrations of a circular ring as developed by Love and Timoshenko has been extended for the case of a circular ring which has radial elastic support and which is subjected to a radial impulse in the plane of the ring. Equations are developed for the frequencies of flexural vibration, and infinite series solutions are obtained for displacements and bending moments with an impulsive load analytically defined as a half-sine wave. Harmonically varying and static loads are also treated. In the development of the theory, the vibrations are assumed to be inextensional, and effects of damping, rotary inertia, and shear are neglected.

The theory was investigated experimentally by tests of a 24-in. diameter ring radially supported by a large number of coil springs. Impulses of half-sine characteristic were delivered by means of a pendulum during which time the force of impact was accurately measured with a dynamometer especially developed for this study. The parameters of elastic support and the duration and intensity of load were varied during the test, and recordings were made of strains and radial displacements as well as external load.

The observed frequencies of vibration were found to agree with those computed by the theory within a few percent up to the seventh mode of flexural motion. Also the observed strains and displacements were found to correlate for the time interval during the pulse and for subsequent free vibrations.

It is concluded that the theory is valid within the bounds of the assumptions provided that the depth of cross section of the ring is small compared with the diameter.

1. INTRODUCTION

The study of free vibrations of a circular ring as developed by Love and Timoshenko has been extended for the case of a circular ring which has radial elastic support and which is subjected to a radial impulse in the plane of the ring.

The fundamental differential equation for the static bending of a thin curved element was established by Boussinesq[1] as follows:

$$M = EI\left(\frac{1}{r+\Delta r} - \frac{1}{r}\right) = \frac{EI}{r^2}\left(\frac{\partial^2 u}{\partial\theta^2} + u\right)$$

The same differential equation was apparently derived independently by Lamb;[2] these solutions may be applied to the bending analysis of a thin circular ring statically loaded in its plane.[3]

The statical bending of circular rings with radial elastic support has been investigated by Pippard and Francis,[4] who also obtained experimental checks by means of static tests of wire wheels.* Similar theoretical analyses have been made by Donnell,[5] and Hetenyi.[6]

Vibrations of a circular ring were first investigated by Hoppe,[7] who derived the frequency equation

$$p_i^2 = \frac{i^2(i^2-1)^2}{1+i^2}\,\frac{gEI}{A\gamma r^4}$$

Love[8] later studied the fundamental equations of motion for both a complete ring and an incomplete ring with a cross section which was also circular. These equations of motion were derived from considerations of the dynamical equilibrium of an element, after neglecting terms for the rotatory inertia and for shear deformations of the ring. Love stated the resulting partial differential equation:

$$\frac{EI}{r^4}\left(\frac{\partial^6 u}{\partial\theta^6} + 2\,\frac{\partial^4 u}{\partial\theta^4} + \frac{\partial^2 u}{\partial\theta^2}\right) = \frac{A\gamma}{g}\,\frac{\partial^2}{\partial t^2}\left(u - \frac{\partial^2 u}{\partial\theta^2}\right)$$

for which the solution was given to be

$$u = \sum_{n=1}^{n=3}\left[C_n \cos i_n\theta + D_n \sin i_n\theta\right]\cos\left(p_n t + \delta\right)$$

If the ring is complete, Love postulated that i_n must be an integer, and that there are vibrations with i_n wave lengths to the circumference, i_n being any integer greater than unity. This result leads to the same frequency equation derived by Hoppe.

---

[1]References are listed on page 68 of this report.

*Instrumentation was confined to Marten's optical extensometers to measure strains in the radial spokes, from which were inferred bending moments and radial displacements of the ring.

For these solutions, the important assumption was made that the center line of the ring is free of any extension. The flexural vibration of a circular ring, when the possible extension of the center line is considered, is discussed by Waltking,[9] and by Federhofer.[10] Vibrations of ring-shaped frames out of the plane of the frame are discussed by Michell,[11] by Love,[8] and by Brown,[12] and torsional vibrations are also treated by Love.[8]

More recently, a mathematical analysis has been given by Carrier[13] of vibrations of a circular ring which is rotating at high speed so as to develop important centrifugal effects and which is either rigidly or elastically supported by radial spokes.

As a further development of the mechanics of circular rings, there is discussed in this paper the dynamical behavior of a ring with radial elastic support subjected to a concentrated radial force. The force-time characteristic is a half-sine wave of duration τ. By application of procedures developed by Timoshenko[14] and Hoppmann[15] for the impulsive loading of straight beams, solutions are derived for bending displacements in the plane of the ring.

The theoretical analysis was investigated experimentally by means of a circular ring 24 in. in diameter which was supported by a large number of radial coil springs intended to simulate a uniform elastic support. The ring was subjected to a radial impulse of controlled duration and intensity during which time the applied force and the strains and displacements were measured with electrical instruments. The ring was also subjected to a harmonically varying force over a continuous frequency spectrum, and the frequencies of flexural vibration were determined by observation of resonance. Since the case of static loading is a limiting case for the dynamic loading, this case was also investigated both theoretically and experimentally.

Several new experimental instruments and techniques were developed for these tests including a means for applying, controlling, and precisely measuring a transient impulse. These are described in detail.

The paper concludes with a comparison of theoretical and experimental results for the various cases of loading.

2. THEORETICAL ANALYSIS

A. STATEMENT OF THE PROBLEM

This investigation pertains to the case of a plane circular ring of constant and symmetrical cross section whose dimensions are small compared with the radius of the center line; one of the principal axes of the cross section is assumed to be situated in the plane of the ring. Further, the ring is considered to have a uniform radial support which is completely elastic and

which exercises constraint only in a radial direction and only as a consequence of radial displacements of the ring. Damping and body forces are neglected in the analysis, and external forces are restricted to radial orientation in the plane of the ring.

B. THE DIFFERENTIAL EQUATION OF MOTION

Consider first an element of the ring as shown in Figure 1. Under the action of the internal shear and normal forces N and B, and flexural moments M imposed by contiguous ring elements, and of the radial and tangential components of particle accelerations, external loads P, and radial elastic support, equations of equilibrium are derived as follows.

In the radial direction, the forces are

$$\frac{\partial N}{\partial \theta} + B = \frac{A\gamma r}{g}\,\frac{\partial^2 u}{\partial t^2} + k\,u\,r - Pr \qquad [1]$$

where k is the modulus of elastic support expressed in units of pounds per inch of circumference per inch radial displacement, and u designates radial displacement taken positive toward the center.

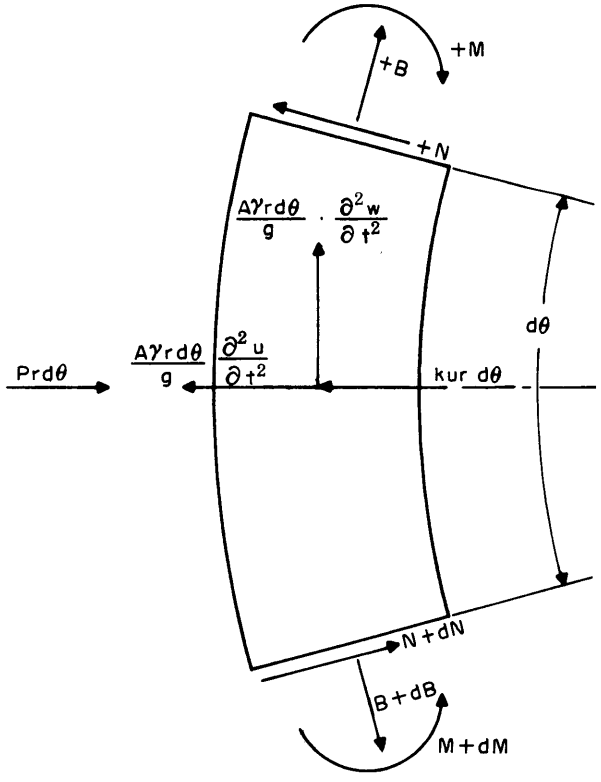

Figure 1 - Dynamical Equilibrium of an Element of an Elastically Supported Ring

In the tangential direction, the forces are

$$\frac{\partial B}{\partial \theta} - N = \frac{A\gamma r}{g}\,\frac{\partial^2 w}{\partial t^2} \qquad [2]$$

where w is the tangential displacement taken positive counterclockwise.

If rotatory inertia is neglected, the equation of equilibrium involving moments is

$$\frac{\partial M}{\partial \theta} + Nr = 0 \qquad [3]$$

It will be noted that terms corresponding to effects of shearing distortion have also been neglected, but the possible error thus introduced has been found by Timoshenko[14] to be unimportant for bars where the wavelength of vibration is at least ten times the depth of cross section.

The tangential displacements w are now assumed to occur in such a form that the extension of the center line is zero. This condition of inextensional vibration was expressed by Love and Rayleigh[16] as

$$u = \frac{\partial w}{\partial \theta} \qquad [4]$$

If the change in curvature in terms of bending displacements is represented by the equation given by Boussinesq[1] for bending of a curved beam,

$$M = EI\left(\frac{1}{r + \Delta r} - \frac{1}{r}\right) = \frac{EI}{r^2}\left(\frac{\partial^2 u}{\partial \theta^2} + u\right) \qquad [5]$$

then, by use of relationships [4] and [5], the equations of equilibrium [1] to [3] may be reduced to eliminate terms of M, N, and B. There is obtained the partial differential equation of motion in terms of tangential displacements:

$$\frac{EI}{r^4}\left(\frac{\partial^6 w}{\partial \theta^6} + 2\,\frac{\partial^4 w}{\partial \theta^4} + \frac{\partial^2 w}{\partial \theta^2}\right) + k\,\frac{\partial^2 w}{\partial \theta^2} - \frac{\partial P}{\partial \theta} = \frac{A\gamma}{g}\,\frac{\partial^2}{\partial t^2}\left(w - \frac{\partial^2 w}{\partial \theta^2}\right) \qquad [6]$$

By differentiating this equation with respect to θ and applying condition [4], an equation may be obtained for the radial displacements:

$$\frac{EI}{r^4}\left(\frac{\partial^6 u}{\partial \theta^6} + 2\,\frac{\partial^4 u}{\partial \theta^4} + \frac{\partial^2 u}{\partial \theta^2}\right) + k\,\frac{\partial^2 u}{\partial \theta^2} - \frac{\partial^2 P}{\partial \theta^2} = \frac{A\gamma}{g}\,\frac{\partial^2}{\partial t^2}\left(u - \frac{\partial^2 u}{\partial \theta^2}\right) \qquad [7]$$

In the usual fashion, it is assured that the radial displacement u is a product of a characteristic function U(θ) and a time function Γ(t):

$$u = U\Gamma \qquad [8]$$

With the variables thus separated, the time function Γ is found by substitution of Expression [8] in Equation [7] to be in the simple harmonic form of circular frequency p:

$$\Gamma = C\cos pt + D\sin pt = \cos(pt + \delta) \qquad [9]$$

This condition yields for the ordinary differential equation of the characteristic function U:

$$\frac{d^6 U}{d\theta^6} + 2\,\frac{d^4 U}{d\theta^4} + \left[1 + \frac{\left(k - \frac{A\gamma}{g}\,p^2\right)}{EI}\,r^4\right]\frac{d^2 U}{d\theta^2} + \frac{A\gamma r^4 p^2}{gEI}\,U = + \frac{d^2 P}{d\theta^2}\left(\frac{r^4}{EI}\right) \qquad [10]$$

The homogeneous equation which corresponds to the freely vibrating ring, when P = 0, is of the form

$$\frac{d^6U}{d\theta^6} + 2\frac{d^4U}{d\theta^4} + \frac{d^2U}{d\theta^2}(1 + \nu - \mu) + \mu U = 0 \qquad [11]$$

in which the coefficients appearing in Equation [10] have been replaced by the symbols ν and μ. The solution of this equation is given by Love[8] to be:

$$U = \sum_{n=1}^{n=3} (C_n \cos i_n \theta + D_n \sin i_n \theta) \qquad [12]$$

where i_1, i_2, and i_3, are roots of the equation

$$i_n^6 - 2i_n^4 + (1 + \nu - \mu) i_n^2 - \mu = 0 \qquad [13]$$

This follows simply from the substitution of Expression [12] in the differential equation [11].

C. FREQUENCY EQUATION FOR FREE VIBRATION OF ELASTICALLY SUPPORTED RING

In the usual dynamical analysis of bars, there would be introduced at this point a statement of the physical boundary conditions from which the constants of integration of the differential equation may be determined. In this problem of a complete ring, however, no such conditions exist for bending displacements or their functions. There does exist, however, the requirement that the solution be univalued in θ. Thus, for a complete ring, there is the recurrence condition that*

$$u_\theta = u_{\theta+2\pi} = u_{\theta+4\pi} \; etc. \qquad [14]$$

This requires that the i_n terms which appear in Equation [12] must be integers, which condition establishes the frequency equation. By employing the explicit coefficients of Equation [10], Equation [13] may be solved for the frequency p_i as

$$p_i^2 = \frac{g}{A\gamma} \frac{i^2}{1+i^2} \left[\frac{EI}{r^4}\left(1 - i^2\right)^2 + k\right] \qquad [15]$$

---

*This condition is not required for an incomplete ring and thus, for such problems, explicit boundary values must be assigned. The problem is discussed by Lamb[2] and, for special cases, is solved by Waltking.[9]

Here, the integer values of i_n are represented simply by i which quantity greater than unity* defines the number of wavelengths to the circumference of flexural vibration.

The solution [12] satisfies the differential equation for all integral values of i and the recurrence condition [14]. This infinite set taken together with frequency condition [15] gives the infinitude of frequencies corresponding to all the normal modes of vibration.

D. RADIAL DISPLACEMENTS AND BENDING MOMENTS CAUSED BY A CONCENTRATED HARMONIC FORCE

The radial displacements and bending moments of the ring in response to external loading $P(\theta, t)$ could be obtained by a solution of the differential equation of motion. However, with the characteristic functions for the normal modes of vibration already determined, it is preferable to solve for the response of the ring by application of LaGrange's equations of motion. This was the approach employed by Timoshenko for the unconstrained ring.[14]

From Equations [9] and [12] the radial displacements may be written in terms of an infinite series, as noted previously.

$$u = \sum_{n=1}^{n=\infty} (C_n \cos i_n \theta + D_n \sin i_n \theta) \cos (pt + \delta) \qquad [16]$$

Since we are considering a single concentrated external force applied at $\theta = 0$, the vibrations must be symmetrical, and consequently the odd functions $\sin i_n\theta$ must not appear in the displacement function. This is accomplished by making the coefficients D_n zero. Then

$$u = \sum_{i=1}^{\infty} a_i \cos i\theta \qquad [17]$$

and

$$w = \sum_{i=1}^{\infty} \frac{a_i}{i} \sin i\theta \qquad [18]$$

where the a_i's are functions of time and are taken as the generalized coordinates.

---

*The case where i equals unity is the case of rigid-body translation of the ring. It should also be noted that for concentrated external loading as treated in this paper, the amplitude of rigid-body motion is limited only by the elastic foundation. For a given value of k, restriction is placed on the magnitude of force P so that rigid-body motion will never be so great as to violate seriously the assumption of pure radial constraint.

LaGrange's equation of motion, which we next apply, may be restated as

$$\frac{d}{dt}\left(\frac{\partial T}{\partial \dot{a}_i}\right) + \frac{\partial V}{\partial a_i} = Q_i \qquad [19]$$

The potential energy V of the system is expressed by

$$V = \frac{1}{2}\int \frac{M^2}{EI}\, ds + \frac{k}{2}\int u^2 ds$$

$$= \frac{EI}{2r^4}\int_0^{2\pi}\left(\frac{\partial^2 u}{\partial \theta^2} + u\right)^2 r\, d\theta + \frac{k}{2}\int_0^{2\pi} u^2 r\, d\theta \qquad [20]$$

By substituting the series solutions [17], there is obtained

$$V = \frac{\pi EI}{2r^3}\sum_{i=1}^{\infty}\left(1 - i^2\right)^2 a_i^2 + \frac{\pi kr}{2}\sum_{i=1}^{\infty} a_i^2 \qquad [21]$$

Similarly, the kinetic energy T of the vibrating ring is

$$T = \frac{A\gamma}{2g}\int_0^{2\pi}\left(\dot{u}^2 + \dot{w}^2\right) r\, d\theta \qquad [22]$$

$$T = \frac{\pi r A\gamma}{2g}\sum_{i=1}^{\infty}\left(1 + \frac{1}{i^2}\right)\left(\dot{a}_i^2\right) \qquad [23]$$

LaGrange's equations [19] then yield

$$\frac{\pi r A\gamma}{g}\left(1 + \frac{1}{i^2}\right)\ddot{a}_i + \left[\left(1 - i^2\right)^2 \frac{\pi EI}{r^3} + \pi kr\right] a_i = Q_i \qquad [24]$$

where Q_i is the external generalized force. This equation reduces to

$$\ddot{a}_i + p_i^2 a_i = \frac{g}{\pi r A\gamma}\left(\frac{i^2}{1 + i^2}\right) Q_i \qquad [25]$$

the solution of which is

$$a_i = E_i \cos p_i t + F_i \sin p_i t + \frac{1}{p_i}\frac{g}{\pi r A\gamma}\frac{i^2}{1 + i^2}\int_0^{t_1} Q_i \sin p_i\left(t_1 - t\right) dt \qquad [26]$$

The constants of integration E_i and F_i depend on initial conditions of displacement and velocity of the ring and are taken here to be zero.

To study now the case of steady-state forced vibration, a radial force P concentrated at $\theta = 0$ is applied with simple harmonic oscillation of frequency ω and maximum intensity P_o .

$$P = P_o \sin \omega t \qquad [27]$$

By calculation of the work done on a generalized coordinate

$$\Delta\, work = P\, \Delta u = P\, \Delta a_i \cos i\, \theta = Q_i\, \Delta a_i \qquad [28]$$

The generalized force Q_i becomes

$$Q_i = P \cos i\, \theta = P_0 \sin \omega\, t \cos i\, \theta \Big|_{\theta = 0} = P_0 \sin \omega t \qquad [29]$$

Thus the transient response corresponding to the particular integral of Equation [26] is given by

$$a_i = \frac{1}{p_i} \frac{g}{\pi r A \gamma} \frac{i^2}{1 + i^2} \int_0^{t_1} P_o \sin \omega\, t \sin p_i \left(t_1 - t \right) dt \qquad [30]$$

By denoting the coefficients by

$$\alpha = \frac{g}{\pi r A \gamma} \; ; \; \beta = \frac{gEI}{\pi r^3 A \gamma} \; ; \; j = \frac{i^2}{1 + i^2} \qquad [31]$$

and integrating, the generalized coordinates or amplitude functions corresponding to the steady-state forced vibration are given by

$$a_i = \frac{P_o\, \alpha\, j}{p_i \left(\omega^2 - p_i^2 \right)} \left(\omega \sin p_i t_1 - p_i \sin \omega\, t_1 \right) \qquad [32]$$

If η_1 is taken as the ratio of forcing frequency ω to the frequency corresponding to any mode of response

$$\frac{\omega}{p_i} = \eta_i \qquad [33]$$

then by Equation [17] the radial displacements are given by

$$u_1 = P_o\, \alpha \sum_{i=1}^{\infty} \frac{j}{p_i^2 \left(\eta_i^2 - 1 \right)} \left(\eta_i \sin p_i\, t - \sin \omega\, t \right) \cos i\, \theta \qquad [34]$$

Similarly, the bending moment M is solved from relationship [5] as:

$$M_1 = P_o \beta \sum_{i=1}^{\infty} \frac{j(1-i^2)}{p_i^2 (\eta_i^2 - 1)} \left(\eta_i \sin p_i t - \sin \omega t \right) \cos i\theta \qquad [35]$$

The time variable t_1 has been changed to t for convenience in notation.

Thus Equations [34] and [35] define the response of the elastically supported ring to a steady-state forced vibration. The frequencies of free vibration are given by Equation [15].

E. RADIAL DISPLACEMENTS AND BENDING MOMENTS WITH TRANSIENT LOADING

There is now examined the response of the system to a transient disturbance defined as a half-sine wave of duration τ and maximum intensity P_o. Following the procedure adopted by Hoppmann[15] for the case of an infinite bar, a harmonic force P' of identical amplitude and frequency ω is superposed on P; see Figure 2. The P' force is initiated 180 degrees out of phase in time with P_1 at a time $t = \tau$, where

$$\tau = \frac{\pi}{\omega} \qquad [36a]$$

The time variable for the force P' is denoted by t', and the following relationships obtain between the time coordinates t and t':

$$t' = t - \tau \quad and \quad t_1' = t_1 - \tau \qquad [36b]$$

where t_1 is the instant at which response is desired to be known.

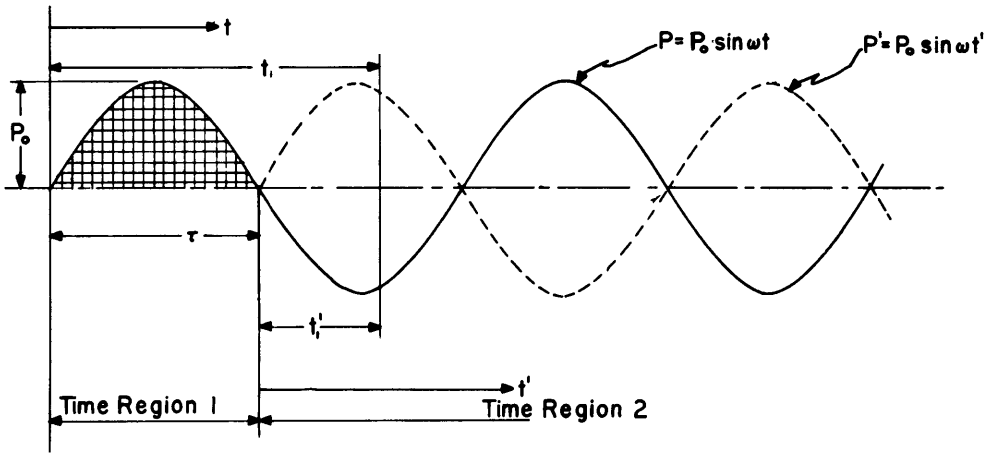

Figure 2 - Schematic Diagram Showing Development of Half-Sine Pulse from Two Superposed Harmonic Oscillations

Treating separately the response of the system to the force P', an expression is obtained for the generalized coordinate a_1' similar to that for a_i given by Equation [32], simply by transformation of the time variable,

$$a_i' = \frac{P_o \alpha j}{p_i(\omega^2 - p_i^2)} \left[\omega \sin p_i (t_1 - \tau) - p_i \sin \omega (t_1 - \tau) \right] \qquad [37]$$

The response of the system after the transient disturbance is obtained by superposing the two steady-state forced vibrations P and P' so that

$$a_i'' = a_i + a_i' \qquad [38]$$

where a_1'' is the new set of generalized coordinates which correspond to the transient force P - P'. By making use of Equations [32] and [36], and noting that

$$\cos \omega\tau = -1 \quad and \quad \sin \omega\tau = 0 \qquad [39]$$

a_1'' becomes

$$a_i'' = \frac{P_o \alpha j \omega}{p_i(\omega^2 - p_i^2)} \left[\left(1 + \cos p_i\tau\right) \sin p_i t_1 - \sin p_i \tau \cos p_i t_1 \right] \qquad [40]$$

The expressions for radial displacement and bending moment, after convenient trigonometric simplification, reduce to

$$u_2 = P_o \alpha \sum_{i=1}^{\infty} \frac{2\eta_i \cos \frac{p_i\tau}{2}}{p_i^2(\eta_i^2 - 1)} j \cos i\theta \sin p_i \left(t - \frac{\tau}{2}\right) \qquad [41]$$

and

$$M_2 = P_o \beta \sum_{i=1}^{\infty} \frac{2\eta_i \cos \frac{p_i\tau}{2}}{p_i^2(\eta_i^2 - 1)} j \left(1 - i^2\right) \cos i\theta \sin p_i \left(t - \frac{\tau}{2}\right) \qquad [42]$$

Again, the time variable has been changed from t_1 to t for convenience in notation.

It will be noted that the response of the ring to a transient pulse is computed for $t < \tau$ by Equations [34] and [35], and for $t > \tau$ by Equations [41] and [42]. The displacements u and bending moments M for the two time

regions corresponding to $t < \tau$ and $t > \tau$ have been marked with the subscripts 1 and 2 respectively.

F. STATIC LOADING TREATED AS LIMITING CASE OF TRANSIENT LOADING

Implicit in this dynamic analysis is the solution for the case of static loading. By consideration of the limiting case where $\omega \to Q$, and $\omega t \to \frac{\pi}{2}$, the radial displacements and bending moments as given by Equations [34] and [35] reduce to

$$u_s = P_o \alpha \sum_{i=1}^{\infty} \frac{j}{p_i^2} \cos i\theta \qquad [43]$$

and

$$M_s = P_o \beta \sum_{i=1}^{\infty} \frac{j(1 - i^2)}{p_i^2} \cos i\theta \qquad [44]$$

The transient response after the disturbance as given by Equations [41] and [42] is, of course, zero.

G. DISCUSSION OF SOLUTION IN SERIES FORM

Equations [34] and [35], which define bending moments and radial displacements during forced harmonic vibration and during the interval of action of a transient half-sine pulse, are in recognizable form. Each term of the series for each of the various modes corresponds to the response of an equivalent single-degree-of-freedom system excited by a generalized force.

It is immediately apparent from Equations [34] and [35] that resonance will occur at any mode when $\eta_1 = 1$; that is, where $\omega = p_1$. If such unique cases are excluded, we can determine convergence by examining separately the various factors which appear in each series term.

With reference first to Equation [34] for displacements--as i increases, p_i increases without limit. Thus

$$\lim_{i \to \infty} \eta_i = \lim_{i \to \infty} \frac{\omega}{p_i} = 0$$

Also,

$$\lim_{i \to \infty} j = \lim_{i \to \infty} \frac{i^2}{1 + i^2} = 1$$

Both cos iθ and sin $p_i t$ remain within the closed interval +1 to -1. Now, by application of the ratio test of succeeding terms, we find Equation [34] converges except where $\eta_1 = 1$. In an analogous fashion, we can find convergence

proved for the bending moments defined by Equation [35] except that the presence of the $(1 - i^2)$ in the numerator of each series term retards convergence.

A similar test of Expressions [41] and [42] for free vibration after termination of a transient also discloses convergence, even where $\eta_i = 1$.

It will be noted that when computing the free vibrations excited in a ring, the factor $\cos \frac{p_i \tau}{2}$ becomes an important modifying term which is very sensitive to small changes in τ, especially at large values of p_i. Consequently, the exact time history of pulse is required for an accurate computation.*

H. COMPARISON OF SERIES SOLUTION WITH A CLOSED-FORM SOLUTION FOR THE CASE OF STATIC LOAD

Inasmuch as the differential equation of the elastically supported ring will yield very easily a closed-form solution with a static load concentrated at $\theta = 0$, an opportunity was provided to check both the accuracy of the derivation and rate of convergence. These closed-form solutions for radial displacements and bending moments are given by Hetenyi,[6] and are reproduced below. Since the solutions are not univalued in θ they must be restricted between the limits of plus π and minus π, but this restriction in no way reduces the utility of a practical solution.

$$u_{s_1} = \frac{Pr^3}{4\lambda\epsilon EI}\left(\frac{2\lambda\epsilon}{\pi\xi^2} - R\cosh\lambda\theta\cos\epsilon\theta + S\sinh\lambda\theta\sin\epsilon\theta\right) \quad ** \quad [45]$$

$$M_{s_1} = -\frac{Pr}{2}\left(\frac{1}{\pi\xi^2} + R\sinh\lambda\theta\sin\epsilon\theta + S\cosh\lambda\theta\cos\epsilon\theta\right) \quad ** \quad [46]$$

where

$$R = \frac{\lambda\cosh\lambda\pi\sin\epsilon\pi + \sinh\lambda\pi\cos\epsilon\pi}{\xi(\sinh^2\lambda\pi + \sin^2\epsilon\pi)} \quad [47a]$$

$$S = \frac{\lambda\sinh\lambda\pi\cos\epsilon\pi - \epsilon\cosh\lambda\pi\sin\epsilon\pi}{\xi(\sinh^2\lambda\pi + \sin^2\epsilon\pi)} \quad [47b]$$

$$\xi = \sqrt{\frac{r^4 k}{EI} + 1} \quad [47c]$$

---

*Salvadori has noted that for a pulse of duration that is short compared with the natural period of vibration, neither the shape nor duration is critical, and that the response depends mainly on the $\int p(t)dt$.[17] In this investigation, the pulses are not confined to those of relatively short duration.

**Compare with equivalent series solution, Equations [43] and [44].

$$\lambda = \sqrt{\frac{\xi - 1}{2}} \qquad [47d]$$

$$\epsilon = \sqrt{\frac{\xi + 1}{2}} \qquad [47e]$$

By application of the closed-form solutions, [45] and [46], and of the series solutions of Equations [43] and [44], computations were made of the bending moments and radial displacements in a ring statically loaded at $\theta = 0$. The dimension parameters correspond to the ring employed in later tests, with a diameter of 24 in. and a 1-in. by 1/8-in. cross section. The series solution was extended through ten terms, and the numerical results of both calculations are given in Table 1. The distribution of static bending moments and radial displacements is shown graphically in Figure 3.

TABLE 1

Static Behavior of Supported Ring as Computed from Both Series and Closed Form Solutions

The ring parameters are k = 6.8, E = 29.2, γ = 0.290, P = 1 at θ = 0.

Orientation		Radial Displacement u mils			Bending Moment M inch-pounds		
Station	Degrees	Series Solution	Complete Solution	Observed	Series Solution	Complete Solution	Observed
1	0	8.911	8.98	7.45*	-1.340	-1.70	-
A	4.7	8.745	-	-	-1.237	-1.24	-1.66
B	23.7	5.687	-	-	0.060	0.002	0.020
D	61.6	-0.962	-	-	0.457	0.413	0.57
E	80.5	-2.316	-	-	0.218	0.290	-
11	94.7	-2.655	-2.43	-3.0	-	-	-
J	175.29	-1.847	-	-	-0.120	-0.110	-0.100
21	189.4	-1.863	-1.84	-	-	-	-

*Observations were made with both inward and outward radial loads and were found to agree.

From a study of Table 1, it is evident that good agreement exists between the two different results, particularly with displacements already expected to have rapid convergence. The extent of agreement for bending moments indicates further the validity of the derived series solutions.

Both results were checked by simple static tests, and the experimental results are also given in Table 1.

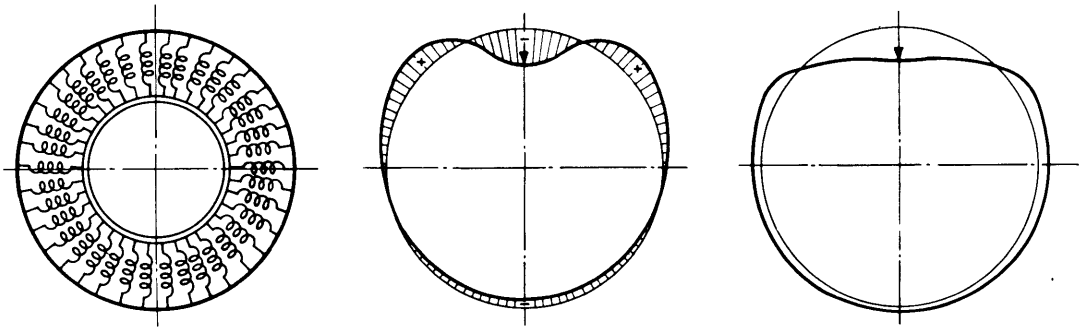

Figure 3 - Bending Moments and Displacements Developed in an Elastically Supported Ring by a Concentrated Static Load

The undistorted ring is shown at the left, bending moment distribution at the center, and deformed ring at the right.

I. NUMERICAL EXAMPLE OF SERIES SOLUTION WITH DYNAMIC LOADING

To test the utility of the derived series solutions, and to provide a numerical basis for evaluation of later experimental work, rather extensive computations have been made of an elastically supported ring with impulsive loading.

For these calculations, the parameters of the problem were assigned the values:

$P = 1$ lb

$r = 12$ in.

$A = 0.125$ in.^{2}

$I = 162.8 \times 10^{-6}$ in.^{4}

$E = 29.2 \times 10^6$ lb/in.^{2}

$\gamma = 0.322$ lb/in.^{3}

$k = 6.8$ and 31.2 lb/in./in.

$\tau = 0.032$ and 0.023 sec

It will be noted that the value chosen for density, γ, includes a correction* for effective mass of the springs, a portion of each of which may be expected to vibrate with the ring.

The frequencies p_i for both rigid-body motion and flexural vibration were computed from Equation [15] and are listed in Table 2. A graphical demonstration of the various modes of vibration is presented in Figure 4.

---

*This correction was applied as follows: The density of the cold-rolled steel was 0.290 lb/in.^{3} and the weight of the ring was 2.73 lb. The springs weighed 0.45 lb of which 2/3 or 0.3 lb was assumed active. Thus the effective density was increased by 11 percent to $\gamma = 0.322$.

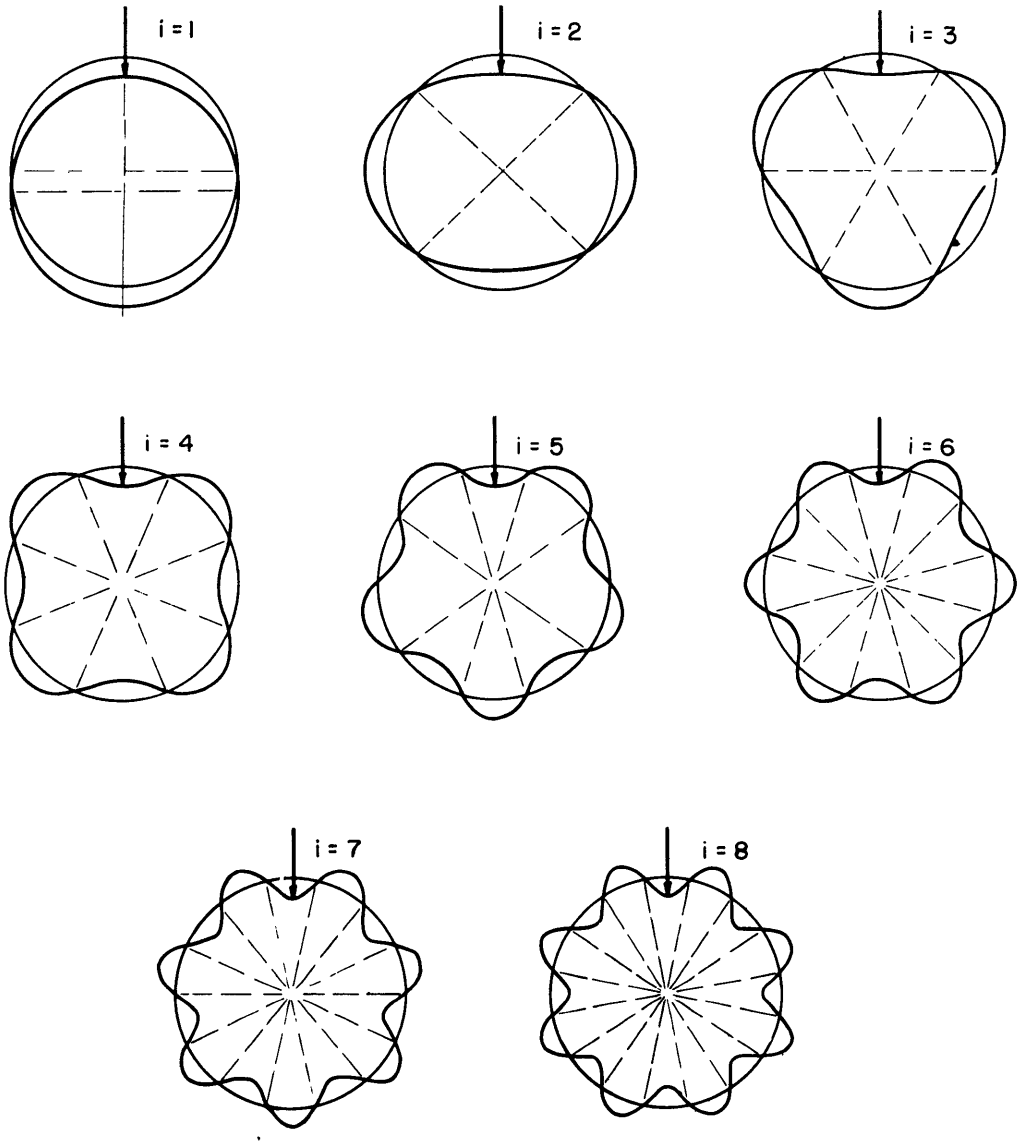

Figure 4 - Schematic Diagram Showing Deformations of Ring for Different Modes of Flexural Vibration

Then, by employing the values for the duration τ of half-sine pulse as actually observed during experiments, the response of the ring was computed for the time intervals both during and after the pulse. The duration τ was 0.032 sec with elastic support of modulus k = 6.8, and 0.023 for k = 31.6.

The bending moments were computed at positions on the ring corresponding to four stations A, B, D, and J, and displacements were computed at Stations 11 and 21; experimental observations also were made at all the stations whose locations are listed in Table 3. The computed contributions of each of the different modes up to i = 7 are plotted in Figures 5 and 6; none were shown where the amplitude was less than 2 percent of the maximum value.

TABLE 2

Frequencies of Free Vibration of Elastically Supported Ring in Cycles per Second

Mode i	Modulus of Elastic Support k = 6.8		Modulus of Elastic Support k = 31.6	
	Computed*	Observed	Computed*	Observed
1	28.74	37.5	62.0	73.8
1'	33.50†	37.5	72.1†	73.8
2	41.49	42.6	80.9	84.8
3	68.50	66.0	100.6	98.9
4	115.5	111.3	138.0	134.7
5	180.0	176.9	195.2	191.9
6	260.7	254.0	271.8	276.5
7	356.8	358.0	365.5	362.0
8	468.2		475.0	474.0

*Computations except for i = 1' were based on the frequency equation [15] for an elastically supported ring with $\gamma = 0.322$ lb/in^3 and $E = 29.2 \times 10^{+6}$ lb/in.^{2}

†Computations were based on rigid-body motion developed for a single-degree-of-freedom system; see Equation [51].

Because the observed frequency of rigid-body vibration was found to differ from the computed frequency, as shown in Table 2, numerical calculations of response were made for i = 1 using observed values of p_i rather than the computed values. The difference in response can be determined from the plots in Figures 5 and 6. An explanation for the failure of computed frequency to agree with the observed is given on page 33 on the basis of the presence in the test apparatus of tangential constraint.

J. DISCUSSION OF RESPONSE PATTERN DURING AND AFTER APPLICATION OF LOAD

It will be noted from an examination of the analysis and of the plotted results that the character of response during the action of the external loads, $t < \tau$, differs from that afterward, $t > \tau$, in one major respect. During the interval of loading the response in each mode is an algebraic sum of two vibrations, one having a frequency ω related to the duration τ of the pulse by $\omega = \frac{\pi}{\tau}$, and a second having a frequency p_i corresponding to the particular mode i of flexural vibration. After cessation of the pulse, however, only free vibrations occur of the frequency p_i.

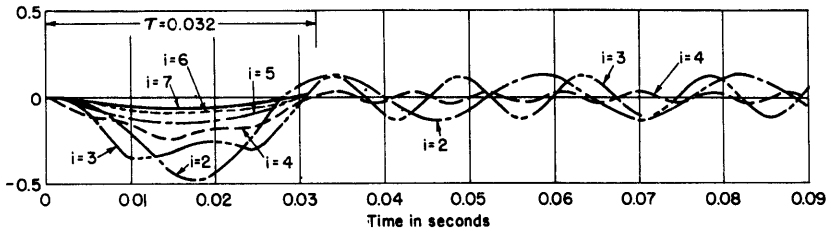

Figure 5a - θ_A = 4.74 Degrees

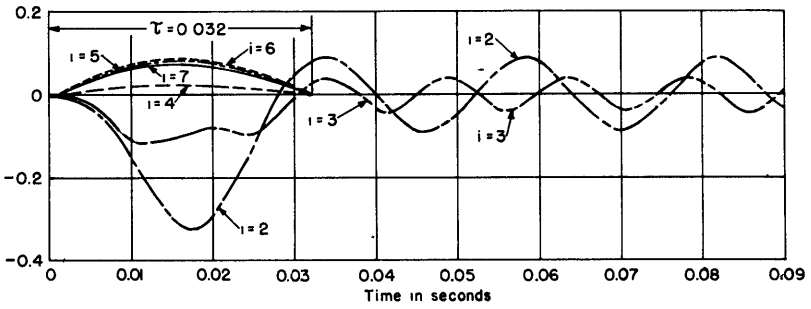

Figure 5b - θ_B = 23.69 Degrees

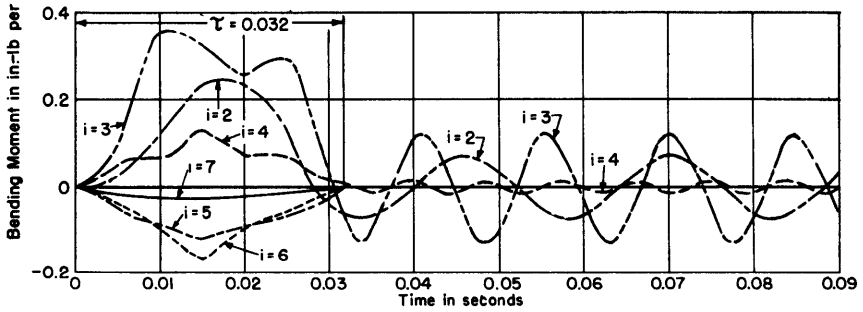

Figure 5c - θ_D = 61.59 Degrees

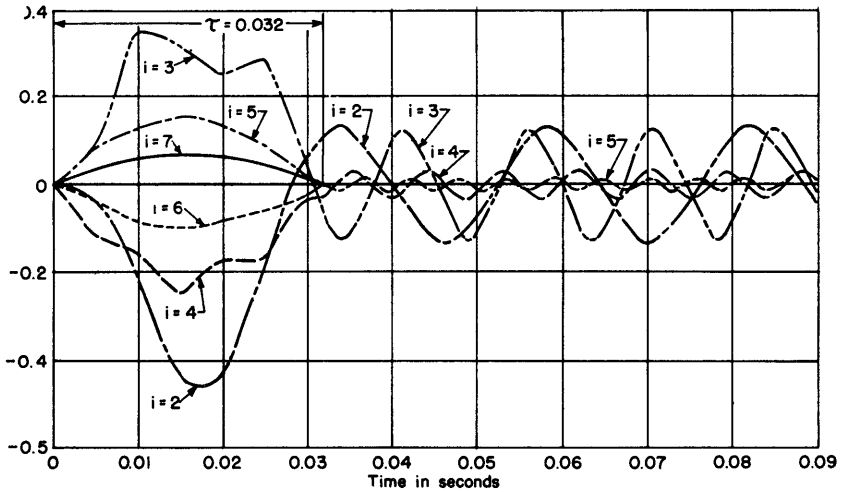

Figure 5d - θ_J = 175.29

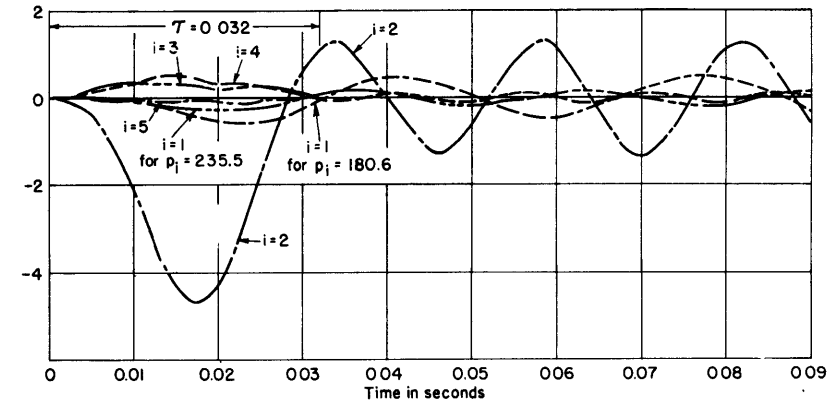

Figure 5e - θ_{11} = 94.74 Degrees

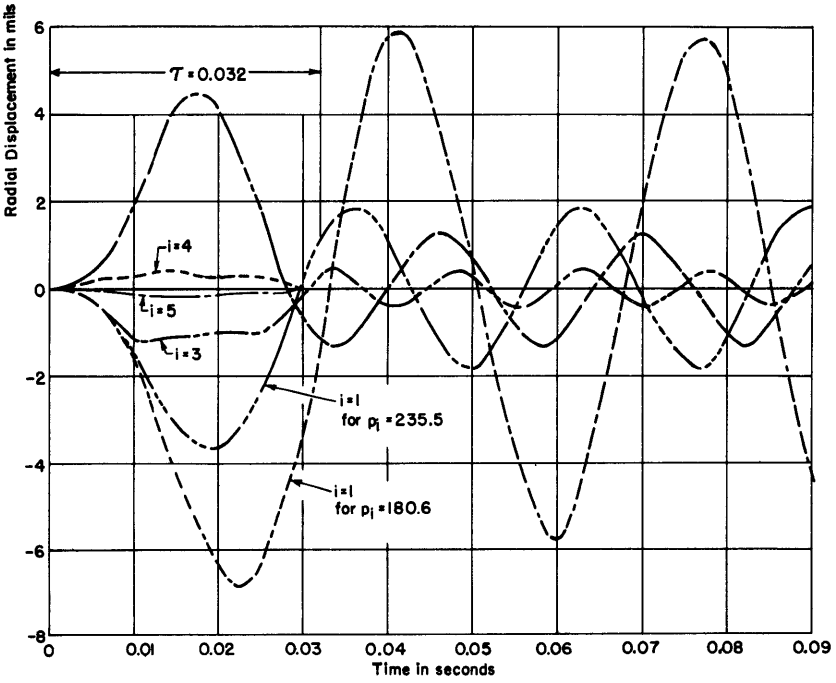

Figure 5f - θ_{21} = 189.47 Degrees

Figure 5 - Computed Response of Ring Showing Contribution of Different Modes for k = 6.8 and τ = 0.032

As was recognized in the analysis, an identity exists between Equations [34] and [41], and [35] and [42] at the end of the pulse, where t = τ; the time derivative likewise corresponds at this instant. This continuity of response for each mode at t = τ is demonstrated in the graphs.

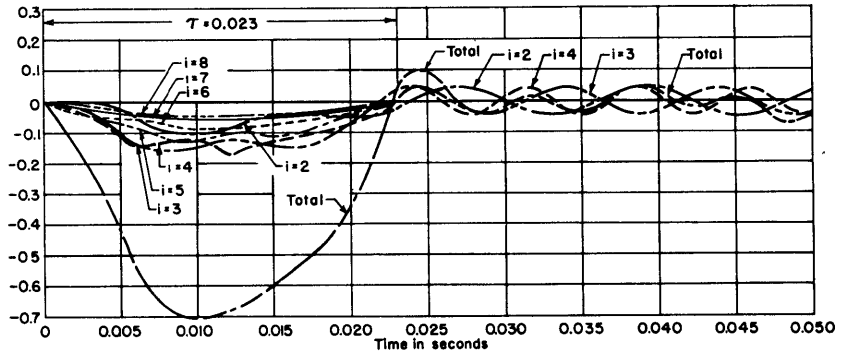

Figure 6a - θ_A = 4.74 Degrees

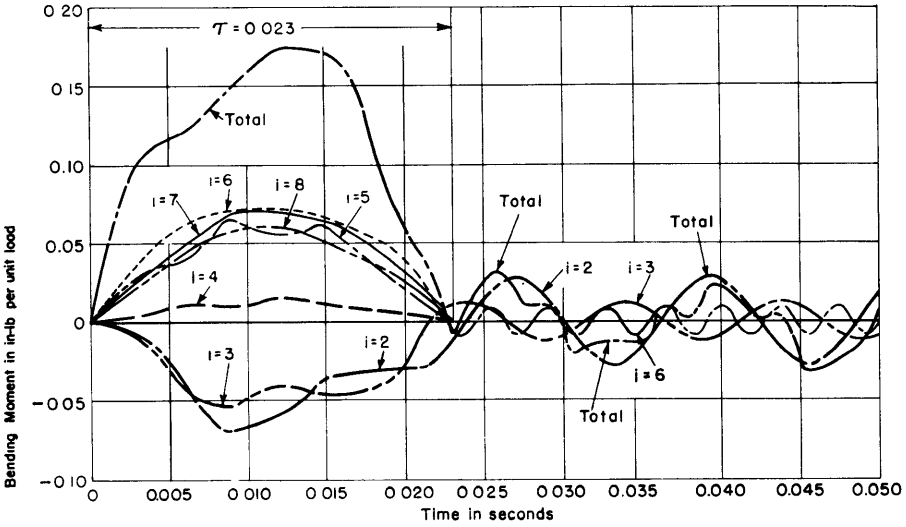

Figure 6b - θ_B = 23.69 Degrees

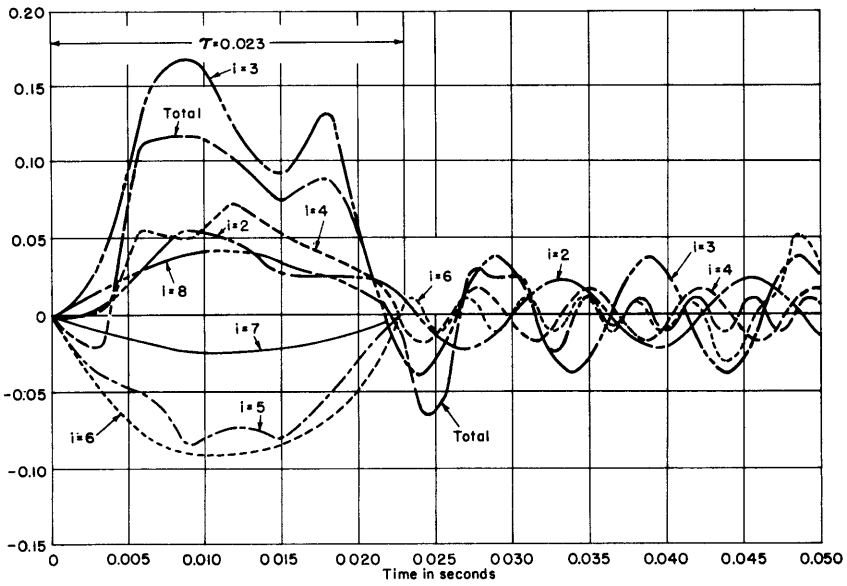

Figure 6c - θ_D = 61.59 Degrees

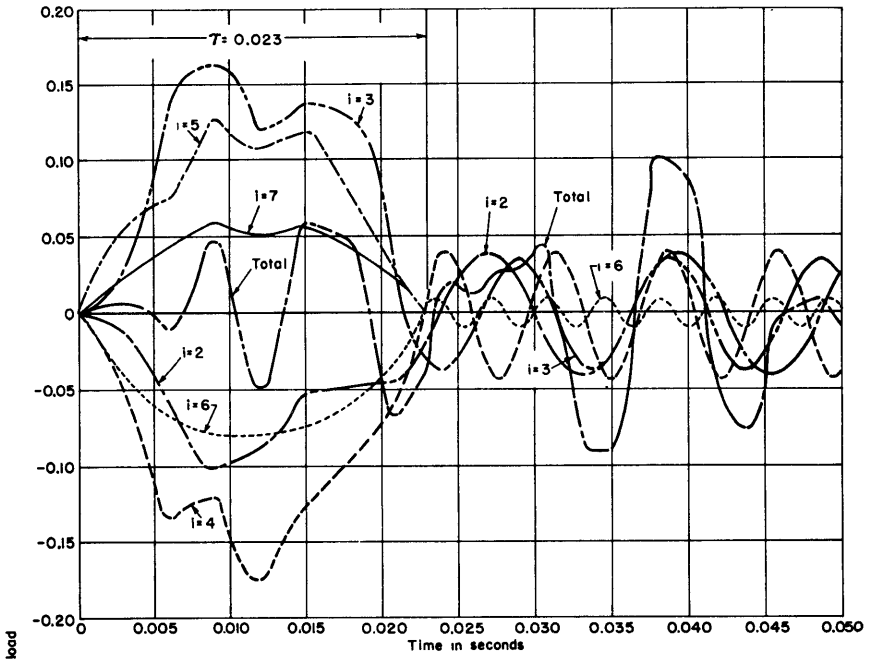

Figure 6d - θ_j = 175.29 Degrees

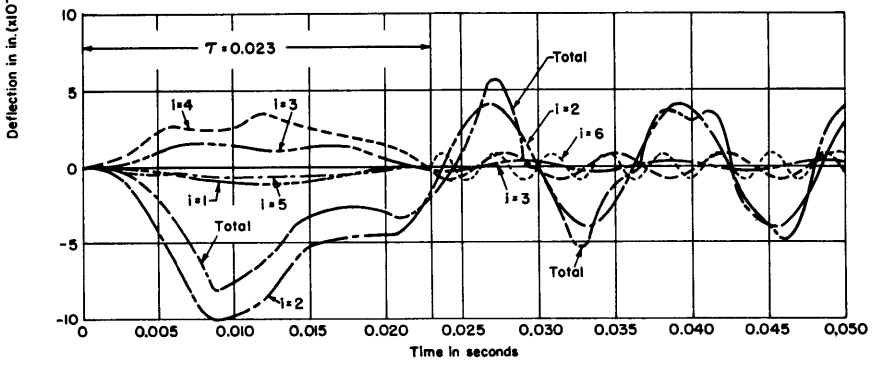

Figure 6e - θ_{11} = 94.74 Degrees

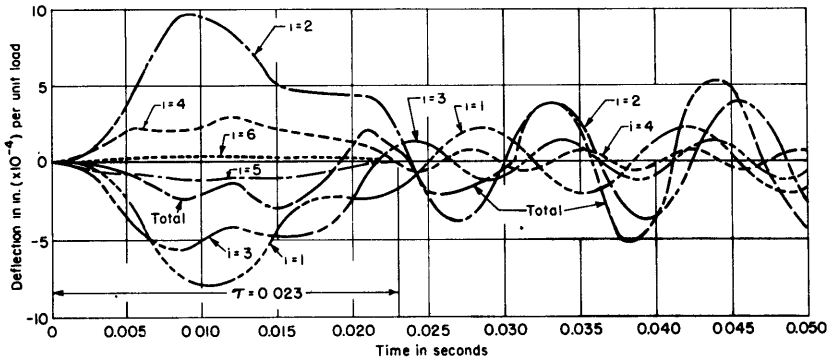

Figure 6f - θ_{21} = 189.47 Degrees

Figure 6 - Computed Response of Ring Showing Contribution of Different Modes for k = 31.6 and τ = 0.023

TABLE 3

Location of Instruments

The angular positions are referred to the line of action of the external force.

Station Designation	Angular Position	
	degrees	radians
Strain Gages		
A	4.74	0.0827
B	23.69	0.4135
C	42.64	0.7442
D	61.59	1.0749
E	80.54	1.4057
F	99.49	1.7364
G	118.44	2.0671
H	137.39	2.3979
I	156.34	2.7286
J	175.29	3.0593
K	260.56	4.5476
L	355.26	6.2004
Displacement Gages		
11	94.74	1.653
21	189.48	3.307

The total response at any time t is the algebraic sum of the contributions from all modes, and plots of the aggregate responses are given later in the report in Figures 18 and 19 when experimental and theoretical results are compared.

3. EXPERIMENTAL ANALYSIS

In the process of analyzing this physical system mathematically, it was necessary to make underlying assumptions so as to render feasible a solution. These assumptions pertain to boundary conditions, to physical constants, and to mathematical operations. Although such assumptions were carefully and rationally formed, the validity of the analysis may remain in doubt because of the critical control which the assumptions may exercise. A collateral experiment was thus desired to confirm the mathematical analysis.

A. STATEMENT OF OBJECTIVES

The experimental investigation was planned with the objective of measuring the dynamical behavior of an elastically supported ring subjected to analytically defined loading. Measurements were desired to determine first the frequencies of various modes of free vibration, and second the response of the ring to a transient pulse of half-sine characteristic.

It has been shown that the transient response is a function of duration τ and intensity P_o of the pulse as well as of the geometry and elastic constraint of the ring. Consequently, for a test specimen of given I, A, and r, it was desired to apply a half-sine impulse and to provide a means of varying the duration τ and the intensity P of loading, as well as the flexibility modulus k of the support.

B. PLANNING OF EXPERIMENT

In order to accomplish these objectives, it was necessary to design an experiment which comprised ont only the test specimen and apparatus for measuring the response of the specimen, but also a pulse generator which could deliver to the specimen a transient having a half-sine characteristic of controllable intensity and duration. A means was also required to measure the applied load. Each of these items is briefly described in this section, and the design and operation of test apparatus are discussed in considerable detail in Appendix 1.

C. DESCRIPTION OF THE RING AND ELASTIC SUPPORT

The ring selected for the test was 24 in. in diameter with a rectangular cross section 1 in. by 1/8 in.; it was manufactured from flat bar stock by rolling a hoop and welding together the two ends. The material was cold-rolled steel with a modulus of elasticity of 29.2×10^6 lb/in.

For test purposes, two different stiffnesses of elastic support for the ring were desired, one to raise the frequency of the first flexural mode of vibration of the unconstrained ring by a factor of two, and a second by a factor of four.

The corresponding required k values were computed to be 6.33 and 31.6 lb/in./in. respectively. After a detailed exploration of various mechanical systems to furnish elastic support, coil springs were selected, oriented radially, and spaced at 2-in. intervals around the periphery. For this arrangement, as shown in Figures 7 and 8, the ring was positioned horizontally,

and its mass was supported by lateral stiffness of the springs. To provide elastic support with radial displacements in both directions, the springs were installed with initial, uniform tension.

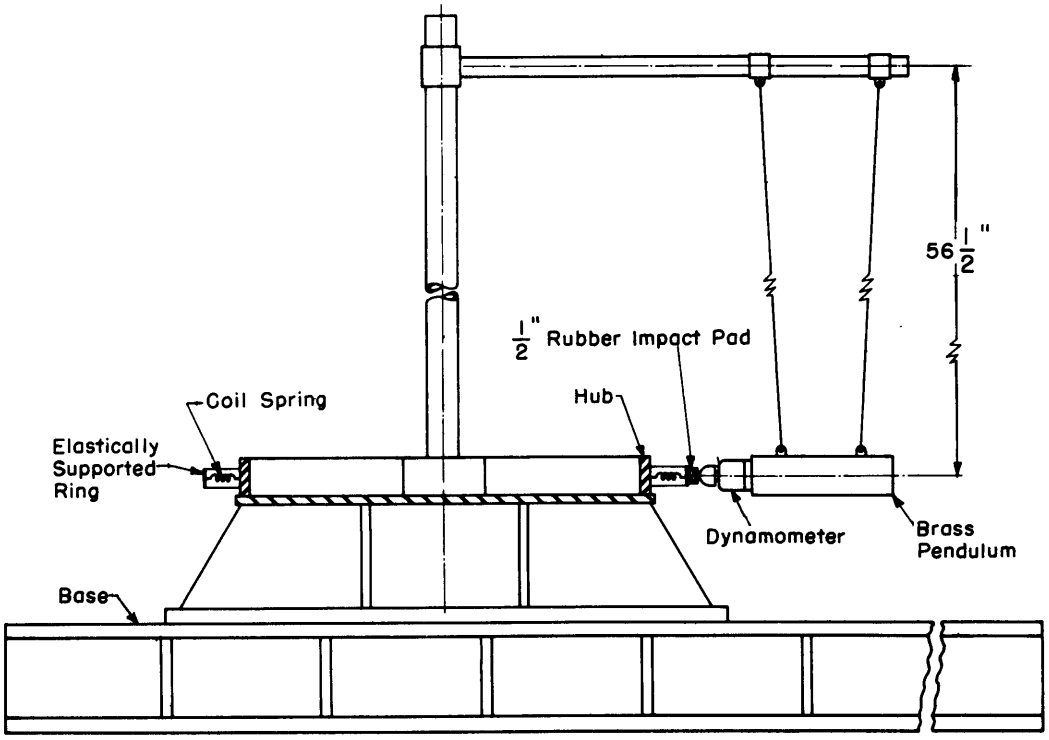

Figure 7 - Schematic Diagram of Test Apparatus

The circular ring is elastically supported in its plane by radial springs attached to a hub and rigid base. Radial impulses are delivered by means of a pendulum, and the applied force is measured with a dynamometer. With this arrangement, a half-sine pulse is developed during impact, and the pulse is made free of all undesirable high-frequency oscillations by the use of a rubber impact pad.

All coil springs were individually calibrated prior to installation to check their stiffness, and it was found that the k values actually obtained were 6.80 and 31.6 lb/in./in. plus or minus 5 percent; these values have been employed in all calculations.

Details of the mechanical design are given in Appendix 2.

D. PULSE GENERATOR FOR APPLYING TRANSIENT LOADS

Because the major development of the theory is for the case of transient loading, a generator was required which could deliver to the ring a controlled radial impulse with a pure half-sine characteristic. Also required was a means for precisely determining the load at the point of impact. In the past, frequent use has been made of a small sphere dropped onto the test

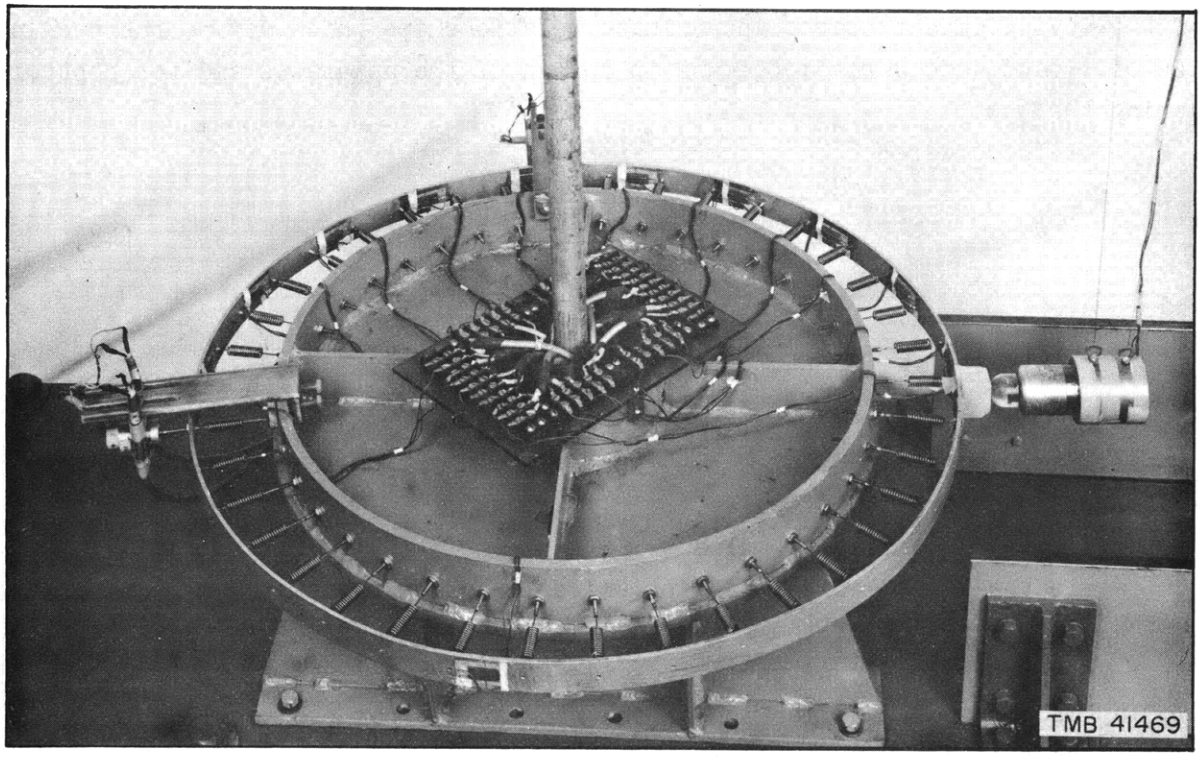

Figure 8 - Arrangement for Direct Loading of Ring by Means of a Pendulum

The ring, 24 in. in diameter, is elastically supported with 38 coil springs oriented radially. The close spacing of the springs is assumed to provide uniform support.

Dynamical response of the ring is measured with wire-resistance strain gages and with differential-transformer displacement gages. The load is measured with the dynamometer mounted on the pendulum.

specimen from a controlled height; and by the application of Hertz's contact theory,[18] computation was made of the duration, intensity, and "shape" of the applied load. This indirect estimate of the impact characteristic may introduce undesirable errors and, further, a limit to the validity of the contact theory occurs when the specimen being struck has diminutive mass or stiffness compared with that of the striking sphere. Also implicit in the theory are short durations of contact compared with the fundamental period of ring vibration. Since longer durations of contact and greater accuracy were desired for this investigation, it was necessary to explore other means of dynamically loading the ring.

From numerous preliminary experiments, it was found that the desired half-sine pulse could be readily developed by striking the ring with a small mass moving at constant velocity. Further, the critical parameters of intensity and duration could be independently controlled as a function of the mass and stiffness of the elastically supported ring and of the mass and velocity

of the moving impact body. Approximate relationships which define the mechanics of impact were derived for use in design of the apparatus and for control during the test.

These were:

$$\tau = \pi \sqrt{\frac{u_s' (W_r + W_p)}{g}} \qquad [48]$$

and

$$P_o = \frac{2 W_p \sqrt{W_p + W_r}}{(2W_p + W_r) \sqrt{u_s' g}} \, \overline{v} \qquad [49]$$

where τ is the duration of pulse,

P_o is the intensity of pulse,

W_r is the lumped weight of ring and coil-spring system,

W_p is the weight of the traveling mass,

$\overline{v}$ is the velocity of the traveling mass, and

u_s' is the static deflection of the ring at the point of application, per unit load.

As will be discussed subsequently, to achieve the desired precision a means was provided for actually measuring the load characteristic, and it was found that the computed durations and intensities were confirmed within 10 percent.

For the tests of the ring, the moving-impact body was designed as a pendulum composed of a cylindrical brass bar 2 in. in diameter, of a length to provide the mass required for a specified loading characteristic. The bar was suspended on phosphor-bronze wires as shown in Figures 7 and 8.

E. THE LOAD DYNAMOMETER

To measure the load developed at impact of the pendulum with the ring, a special dynamometer was developed which permitted remote electrical recording of the load simultaneously with other measurements of response. This dynamometer was designed as a short cylindrical tube, 1/2 in. in diameter with a wall 1/100 in. thick; it was fitted with electrical strain gages oriented for maximum response to axially applied load and provided with a concentric aluminum shield for mechanical protection of the gages (see Figure 9). The dynamometer was calibrated statically, and its response was found to be linear and completely free of temperature instability. Its sensitivity was 2.37 μin./in./lb of load which permitted the measurement of forces as small as 5 lb. The natural frequency was high enough to ensure faithful detection of forces with durations as short as 0.01 millisecond.

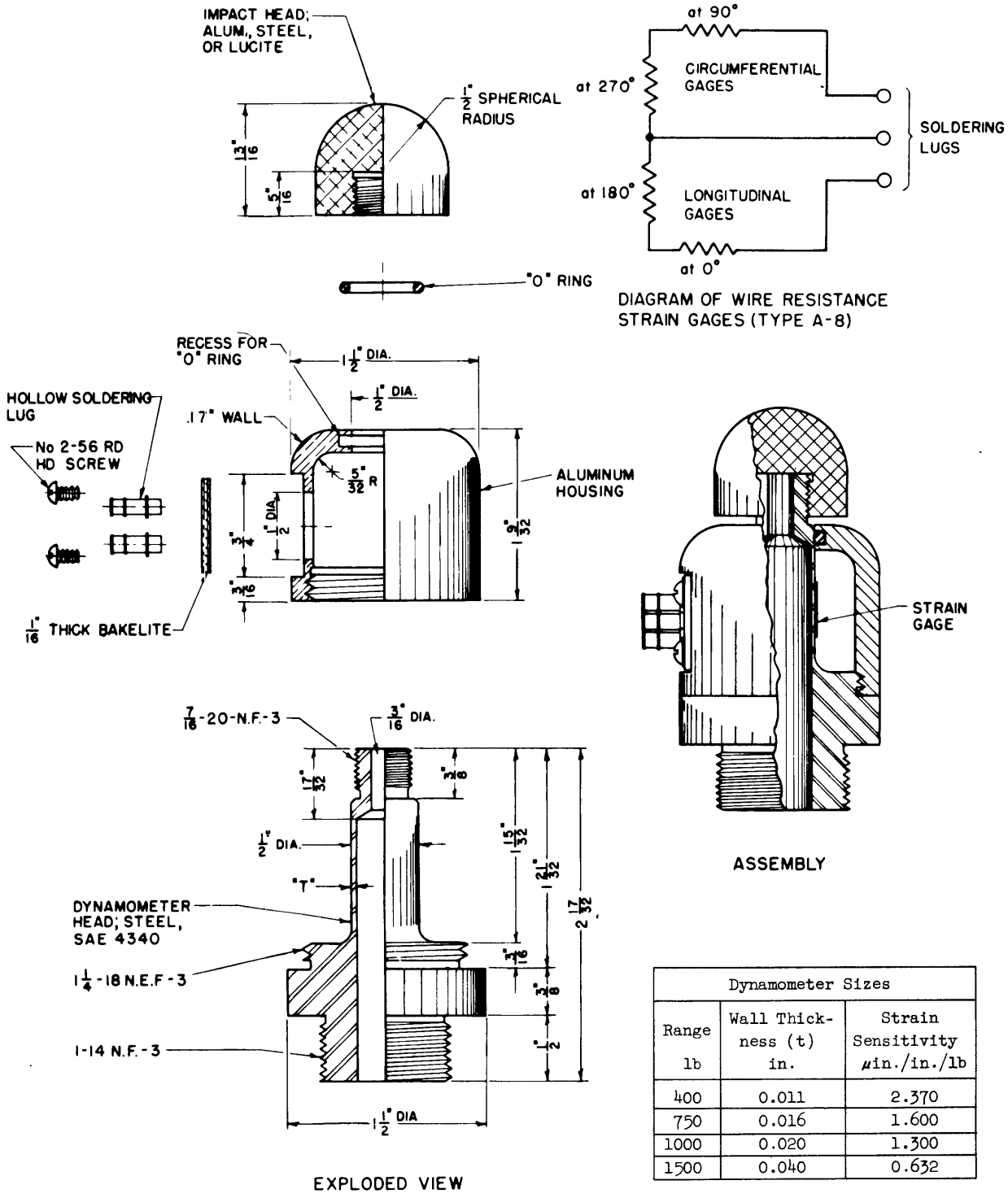

Dynamometer Sizes		
Range lb	Wall Thickness (t) in.	Strain Sensitivity μin./in./lb
400	0.011	2.370
750	0.016	1.600
1000	0.020	1.300
1500	0.040	0.632

Figure 9 - Construction Details of the Load Dynamometer

The force of impact was measured with strain gages mounted on a hollow tube which would be axially loaded. Orientation of gages was selected to minimize sensitivity to bending and torsion of the tube and to temperature effects.

The instrument sensitivity depends on wall thickness as shown in the table, and the natural frequency depends on the length. For this instrument it was in excess of 50,000 cps.

With the strain-gage components used in this dynamometer, any auxiliary amplifying system may be employed which is ordinarily adapted to electrical strain-gage systems. For these tests, a TMB Type-1A strain indicator[19] was used because of its great sensitivity. It operates on a carrier frequency of 2200 cps and has a linear response from 0 to 200 cps, which was ample here where durations of load always exceeded 15 milliseconds.

F. EXCITATION OF STEADY-STATE FORCED VIBRATIONS

Early tests with transient loading revealed that the various frequencies of flexural vibration could not be distinguished on records of response so that an independent means was required to measure these frequencies. Resort was made to a heavy-duty loud-speaker element attached to the ring and excited by an audio oscillator. Resonance was very easily detected from audible sounds from the vibrating ring as well as by visual observation of strain-gage signals, and driving power was sufficient to excite the eighth flexural mode without difficulty.

G. INSTRUMENTATION TO MEASURE STRAIN AND DISPLACEMENT

The response of the ring was considered definable in terms of bending moment and radial displacements and instrumentation was provided for their measurement.

The bending moments were measured by wire-resistance strain gages, mounted in pairs on both faces of the ring at each station so as to double the electrical output and ensure temperature compensation. Gage locations are shown in Figure 10. The measured strains e were converted to units of bending moment by the relationship $M = \frac{1}{2} \frac{IeE}{c} = 0.038\ e$ where the factor 1/2 was introduced to account for the doubled strain indication from two gages.

Strain signals were obtained by the use of the TMB-1A amplifier equipment which incorporates an alternating-current source for the strain gages and an amplifier and power output to drive a string galvanometer. The units also include a calibration system.

Radial displacements were measured with Schaevitz transformer gages [20] These consist of a primary energized with alternating current and two secondary coils wound on a hollow tube and differentially connected. A small steel core free to move in the tube produces an electrical output whose voltage is proportional to motion of the core relative to the transformer. These gages were used with an auxiliary driving unit[21] which furnishes 1000-cycle alternating current to the gage and includes sense-discriminating and rectifier circuits which give a d-c output (with a sense of direction) proportional to motion of the core.

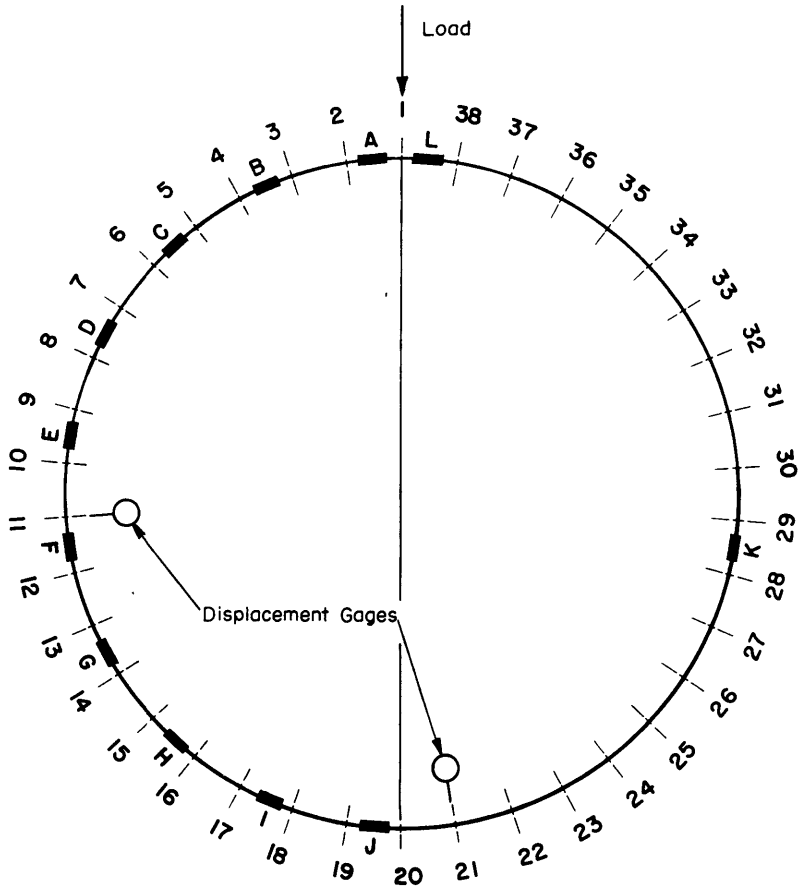

Figure 10 - Location of Strain and Displacement Gages

The numbers indicate spring locations; the letters indicate strain gages.

The gages were calibrated after they were in place by means of a mechanical device with a dial indicator.

H. RECORDING EQUIPMENT

A Consolidated engineering string oscillograph Type 5-101B was employed for recording amplified electrical signals from the various pickups. A 60-cps signal was also recorded as a timing trace. The arrangement of apparatus is shown in Figure 11.

4. EXPERIMENTAL RESULTS AND COMPARISON WITH THEORY

In this section, the important experimental results are summarized and compared with the theoretical solutions for several cases of impulsive loading, and it is on the basis of this correlation that the validity of the analysis hinges.

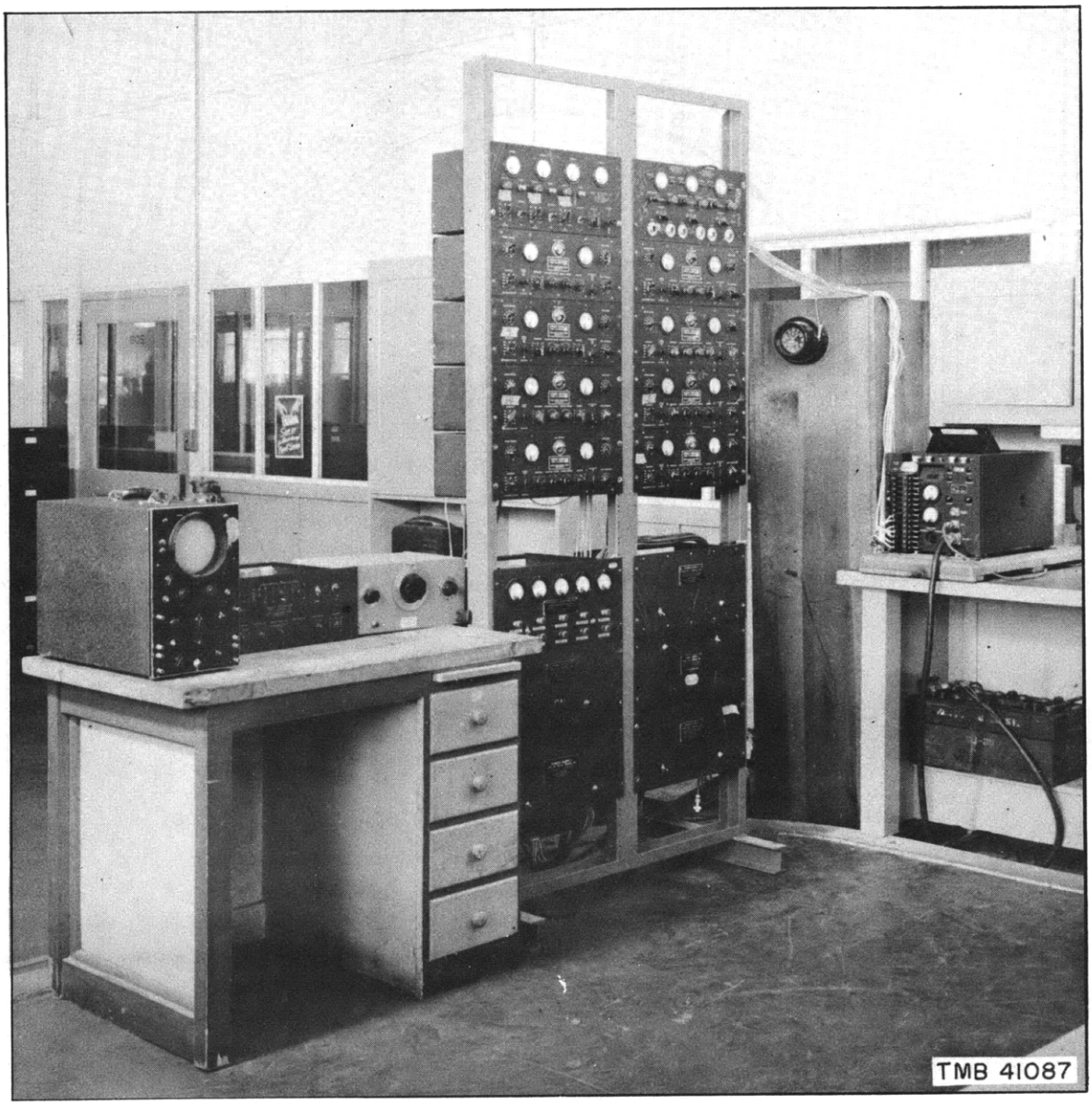

Figure 11 - Auxiliary Electronic and Recording Equipment

Eight TMB Type-1A strain indicators with power supplies are mounted in the relay racks, together with one 5-channel differential transformer driving unit (middle of left rack). The Consolidated string oscillograph for recording is shown at the right, and a cathode-ray oscilloscope with external-sweep generator is shown at the left of the racks.

A. TEST PROCEDURES

A large number and variety of tests were performed with controlled dynamic loading and frequent repetition of early tests was required because the importance of the rubber impact pad had not been determined and the observed sine pulse was erratic; further, until the criteria were established by which the character of transient loading was evaluated, the duration and intensity of load could not be controlled. Also with the preliminary tests, the amplitude of response could only be estimated so that the gain settings and adjustments required of the auxiliary equipment had not been established at values to produce optimum height of records. All these difficulties were resolved during preliminary tests, and the final results are given in the following subsection.

Tests were conducted usually with the assistance of a second person. First the equipment was turned on and allowed to heat for an hour so as to ensure stability. A check was made of resistance to ground of strain gages and of satisfactory operation of displacement gages. The indicators were balanced, and the string oscillograph was checked to note the intensity of noise levels. Gain settings were adjusted, and illumination intensity and proper operation of timing lines were checked on the oscillograph. Then the test was performed by releasing the pendulum on a prearranged signal. The oscillograph motor was started one second before impact to guarantee uniform paper speed. Photographic records were developed after each test to determine possible malfunctioning before continuing the experiment.

B. RESULTS OF STEADY-STATE VIBRATION TESTS

The procedure for applying a steady-state forced vibration over a wide frequency range to determine the natural frequencies of vibration is described on page 61. These tests were conducted with two different stiffnesses of springs, and samples of the oscillograms of strains recorded at resonance for various modes of flexural vibration are shown in Figures 12 and 13. The frequencies of vibration corresponding to these states of resonance for two different constants of elastic support are given in Table 2 where are also listed the frequencies as computed from Equation [15], see page 17.

C. COMPARISON OF OBSERVED AND COMPUTED FREQUENCIES OF FREE VIBRATION

For all the flexural modes up to the seventh, i.e., for $i > 1$, the agreement between the observed and computed values is excellent. Such a correlation with the use of two different values of elastic support k was interpreted as reassuring evidence of the validity of the theory and also of the

satisfactory mechanical arrangement of the supported ring. This is one of the most important results of the experiment.

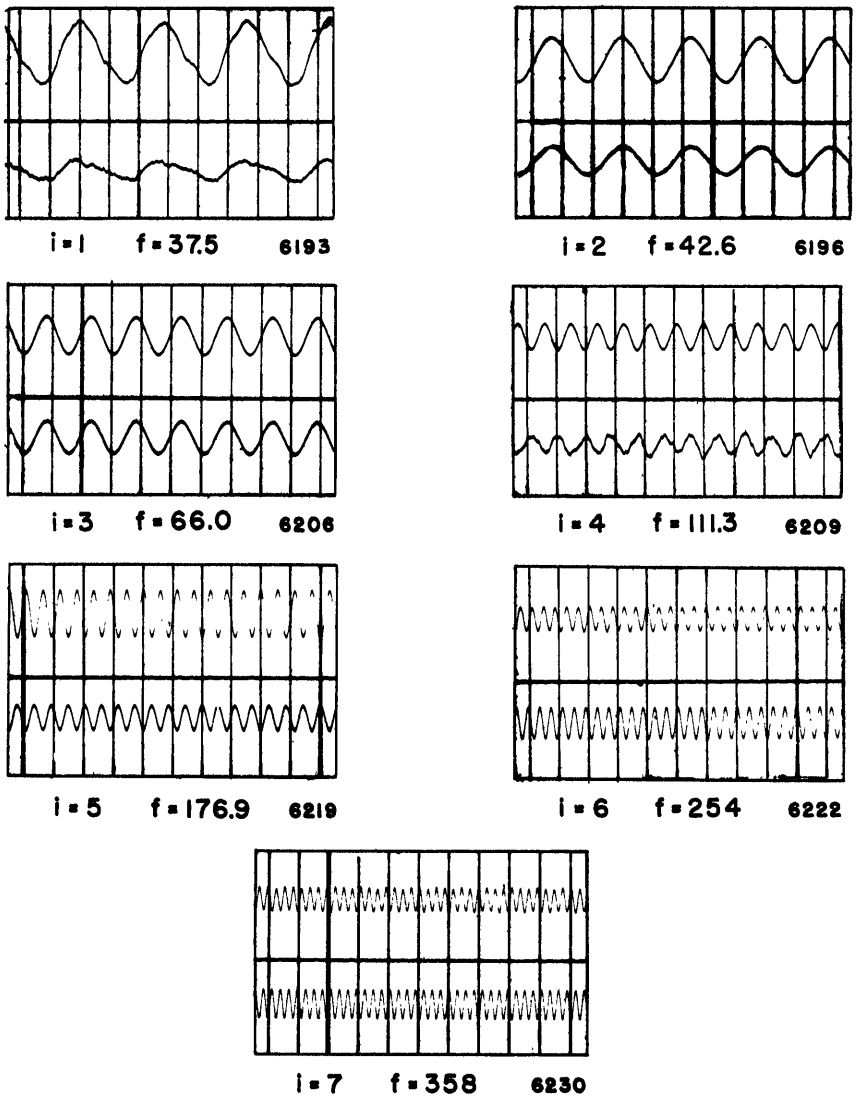

Figure 12 - Oscillograms with Steady-State Forced Vibration, k = 6.8 lb/in./in.

D. DISCUSSION OF RIGID-BODY TRANSLATION AND THE PRESENCE OF TANGENTIAL CONSTRAINT

One obvious discrepancy in frequencies is noted in the case of rigid-body translation, where i = 1. Prior to any tests, a calculation of rigid-body translation of the ring was made by the following simple procedure, with the assumption that all springs were lumped to one of constant K.

$$K = \sum k_n \cos \theta_n = 4 k_n r \int_0^{\frac{\pi}{2}} \cos \theta \, d\theta = 4 k_n r \qquad [50]$$

$$p_i' = \sqrt{\frac{Kg}{2\pi r A \gamma}} = \sqrt{\frac{2}{\pi}} \sqrt{\frac{k_n g}{A\gamma}} \qquad [51]$$

where p_i' is the circular frequency of rigid-body motion, and k_n is the stiffness constant associated with each individual spring. In this derivation of rigid-body motion, there is taken into account the capacity of a radial spring to exert tangential constraint. As shown in Table 1, the frequency of vibration p_i' as obtained with this computation is in better agreement with the observed frequency than with the value computed by using Equation [15]. In the

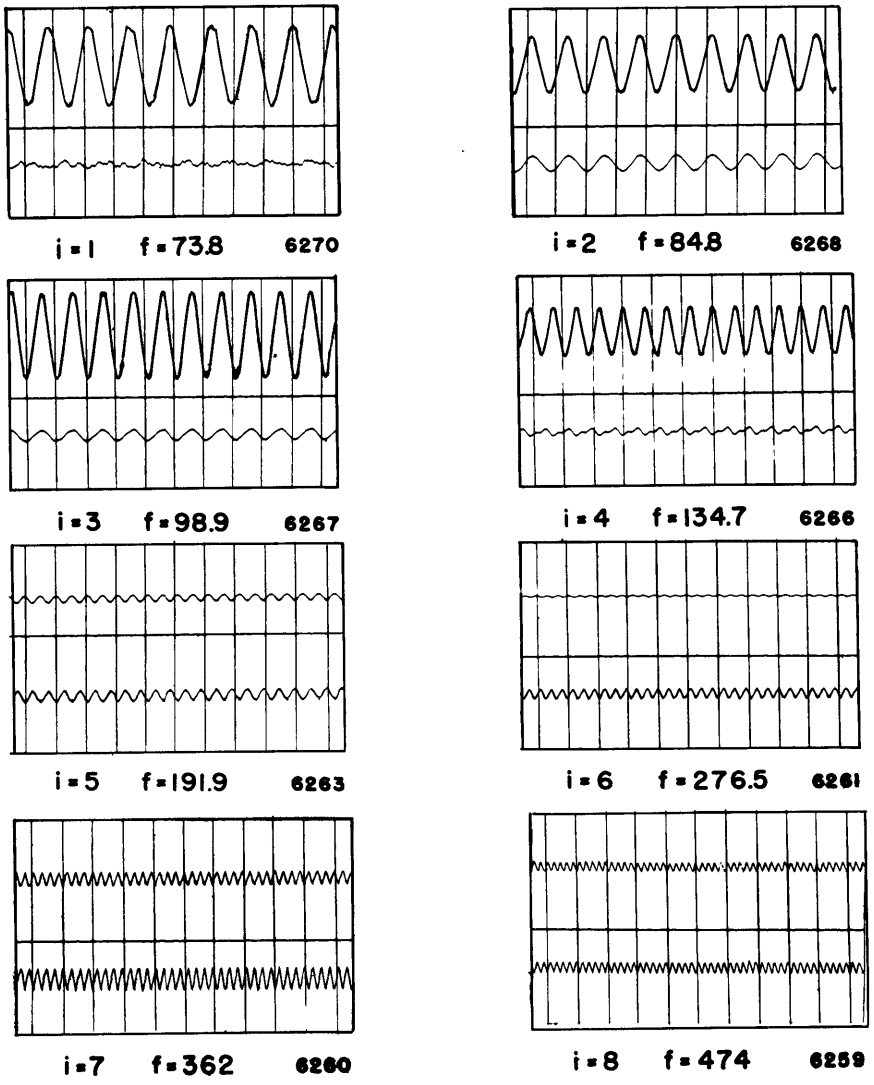

Figure 13 - Oscillograms with Steady-State Forced Vibration, k = 31.6 lb/in./in.

theoretical analysis it was assumed that only radial elastic support could occur with radial displacement, but in the test it is believed that the coil springs offered additional tangential support. Thus the simplifying assumption was not experimentally achieved, and the difference between computed and observed frequencies for the case of rigid-body motion is explained.

This discrepancy prompted an additional analysis of the ring with tangential elastic support, results of which will be given in a subsequent report. Of significance here is the frequency equation which was derived in the same fashion as Equation [15], with the addition of a term corresponding to tangential support of modulus m. The modified frequency equation is

$$p_i^2 = \frac{1}{1+i^2}\,\frac{g}{A\gamma}\left[\frac{EI}{r^4}\,i^2\,(1-i^2)^2 + k\,i^2 + m\right] \qquad [15a]$$

It is apparent that for i = 1 corresponding to rigid-body translation, the tangential and radial supports exercise equal influence on the frequencies, but with higher modes the i^2 factor for k would evoke its predominance. This relationship serves to explain why the presence of tangential constraint in the experimental apparatus caused disagreement between computed and observed frequencies only in the mode for i = 1. If, however, m were far greater numerically than k, considerable effect would be observed at the lower modes of flexural vibration—but then the problem would be one essentially of a ring with tangential instead of radial support.

In the computation of the response of the ring, the frequency corresponding to rigid-body motion is of some significance for radial displacements but not for the bending moments because the i = 1 term does not appear in the moment equation. To rectify the error in displacements, which would appear if rigid-body frequencies given by Equation [15] were employed, the frequency of rigid-body motion may be computed according to the elementary solution given by Equation [51] or, if m is known, by Equation [15a]. This procedure in no way vitiates the main body of the theory.*

E. TESTS WITH TRANSIENT LOAD

Transient loading of the ring was produced by dropping a pendulum of selected mass through a predetermined stroke. Although not presented in detail here, for each combination of pendulum weight, spring support, and thickness of rubber pad it was observed that with different strokes the duration of load remained essentially constant and that the magnitude varied in direct

*It will be noted that with tangential constraint, an analysis of response of the ring yields equations identical to Equations [34], [35] and [41] to [44] except that p_i is computed by Equation [15a] instead of [15].

proportion to the stroke. Sometimes, minor variations in time history occurred, but the character of the half-sine pulse was maintained. The successful achievement of this shape pulse is one of the critical phases of the entire experiment.

During transient-load tests, there were recorded simultaneously the indications of load, strain at seven stations, deflections at two stations, and a 60-cps timing pulse. By using the height of calibration steps recorded prior to each dynamic test, scales were established for these various quantities. Shown in Figures 14 to 17 are four typical oscillograms.

The variety in character of response at different stations is immediately apparent. Near the point of application of load, Stations A and L, the bending moments during loading are similar in pattern to the loading pulse; whereas elsewhere irregular undulations appear. The delay in incidence of response at stations remote from the point of impact is also apparent.

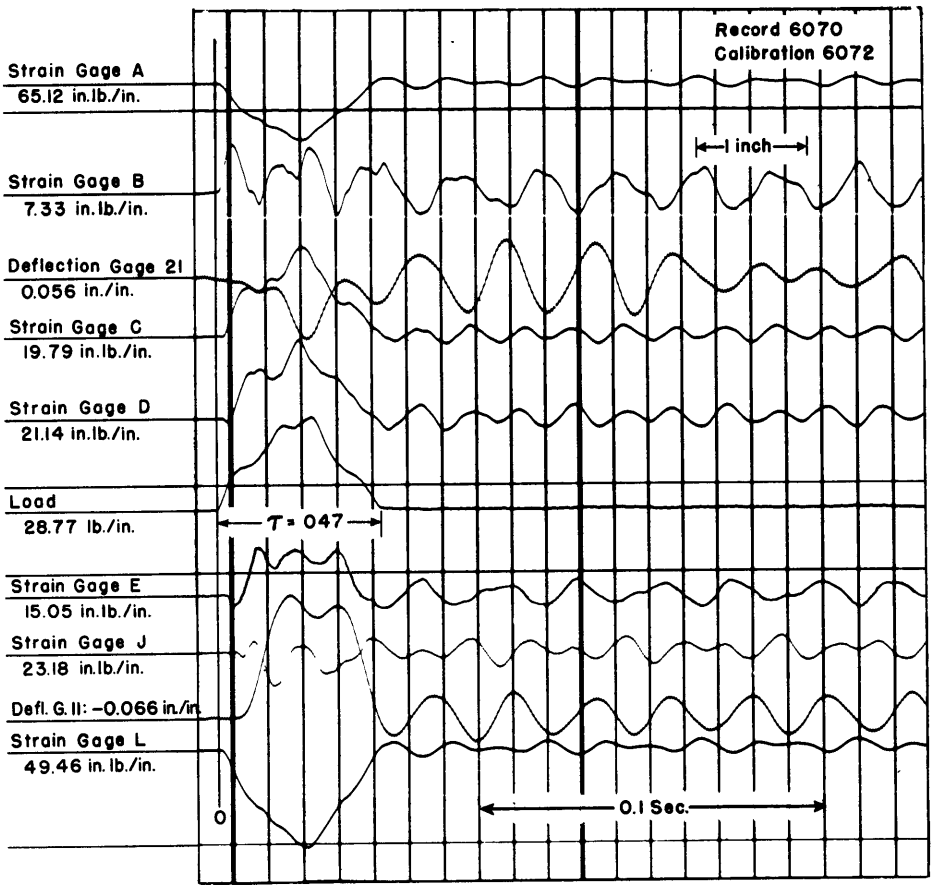

Figure 14 - Oscillogram of Ring Response with $k = 6.8$ and $\tau = 0.047$

Force was applied directly by a 5-lb pendulum with a 10-in. stroke. The scale for each trace is given at the left.

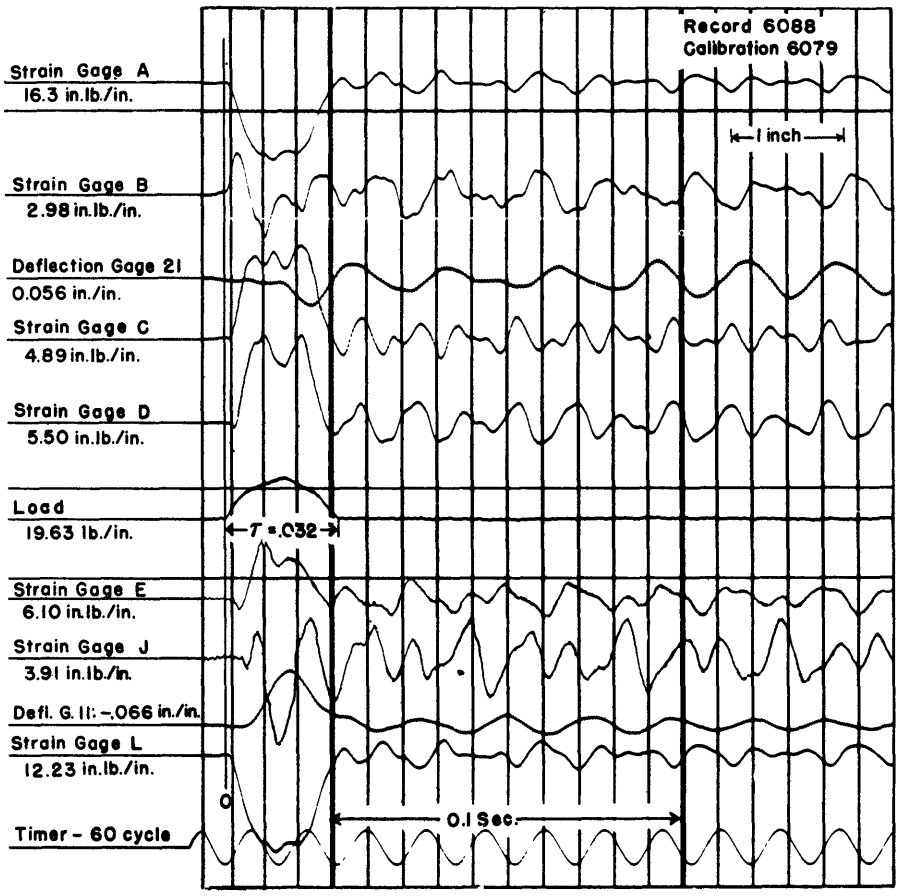

Figure 15 - Oscillogram of Ring Response with $k = 6.8$ and $\tau = 0.032$

Force was applied directly with a 2.21-lb pendulum with a 6-in. stroke.

It will be noted that at some locations, response during the pulse greatly exceeds the subsequent free vibrations, and the relative amplitudes depend on the location of the point at which measurements were observed. It will also be noted that few, if any, regular periodic fluctuations are observed which correspond to any of the frequencies of various modes of flexural vibrations. This character of response was not the result of damping because high-frequency oscillations, at least up to frequencies as great as 400 cps, were found to persist for at least 0.5 sec—long after cessation of the pulse. Thus, of some significance is the presence of the contribution of higher modes of vibration without evidence of sharp fluctuations in response of frequencies corresponding to these modes.

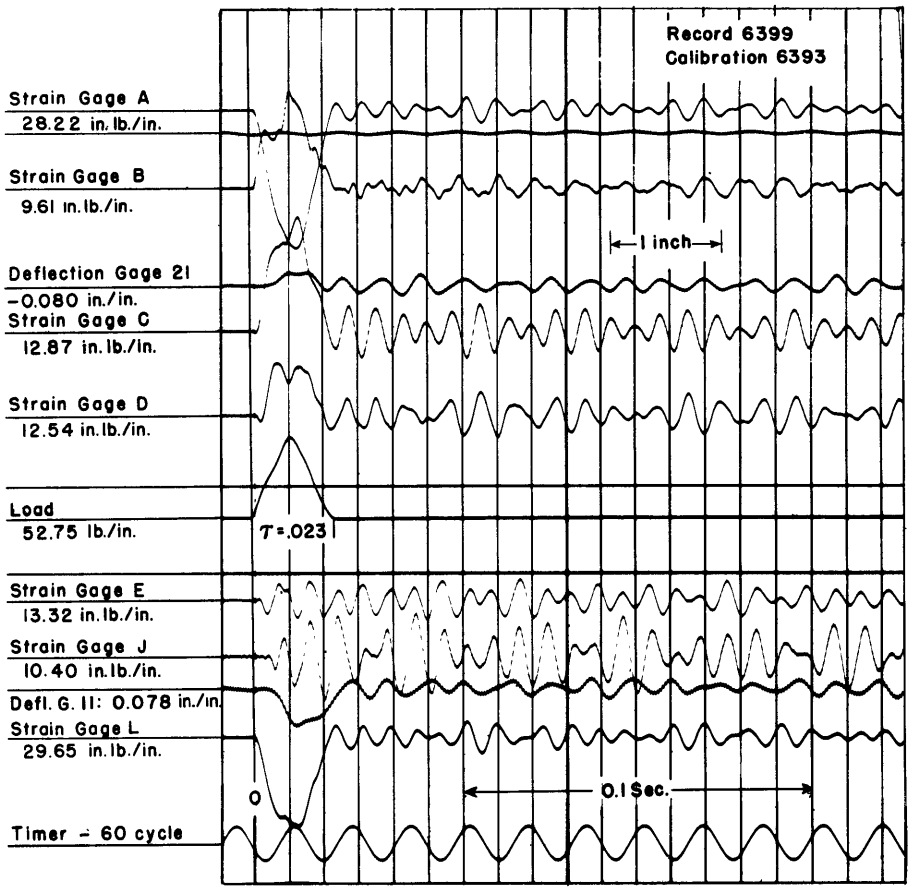

Figure 16 - Oscillogram of Ring Response with k = 31.6 and τ = 0.023

Force was applied directly with a 2.21-lb pendulum with an 18-in. stroke.

F. COMPARISON BETWEEN OBSERVED AND THEORETICAL STRAINS AND DISPLACEMENTS

A number of these photographic oscillogram records have been employed for comparison with the theoretical response; these records were reproduced point for point with only an appropriate change in scale to provide uniformity. They are plotted as solid lines in Figures 18 and 19.

Plotted as broken lines are the aggregate responses as previously computed by the theory, for which the contributions of various modes were plotted separately in Figures 5 and 6.

It is apparent that an encouraging degree of agreement between the computed and observed behavior is found both during and after the transient disturbance. Not only are the intensities of response comparable, but similar patterns are found in both the experimental and computed curves.

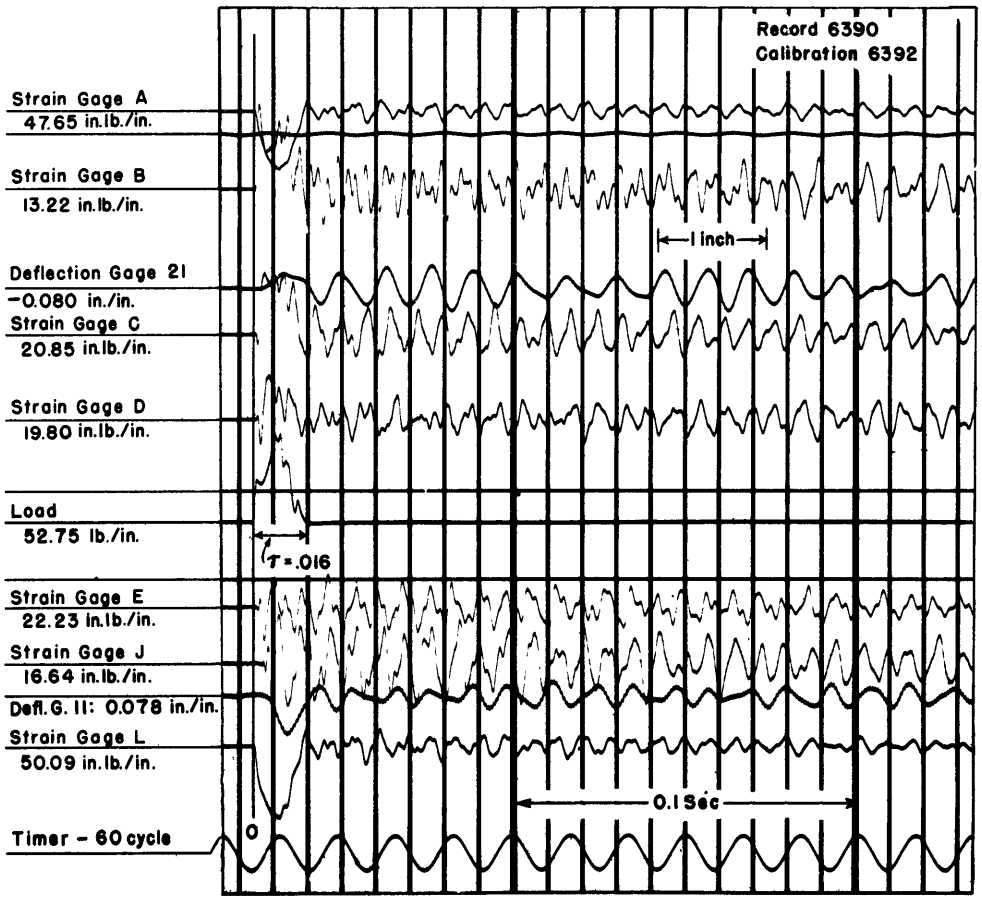

Figure 17 - Oscillogram of Ring Response with $k = 31.6$ and $\tau = 0.016$

Force was applied directly with a 2.21-lb pendulum with a 12-inch stroke. Here the rubber impact pad was omitted so as to observe effects of its omission.

Obviously the extent of agreement is significant from the point of view of both confirming the theory and for demonstrating that experimental techniques were satisfactory.

G. DISCUSSION OF LINEAR RESPONSE WITH RESPECT TO INTENSITY OF LOAD

The patterns of response demonstrated between different strain and displacement gages were noted to change only in amplitude with change in stroke of pendulum; with the same strokes, records could be repeated within 5 percent. Further, a careful check of numerous records showed that all amplitudes of a response were in direct proportion to the intensity of the applied load. Thus verification was obtained of the linear relationship between radial displacement and bending moment with the load.

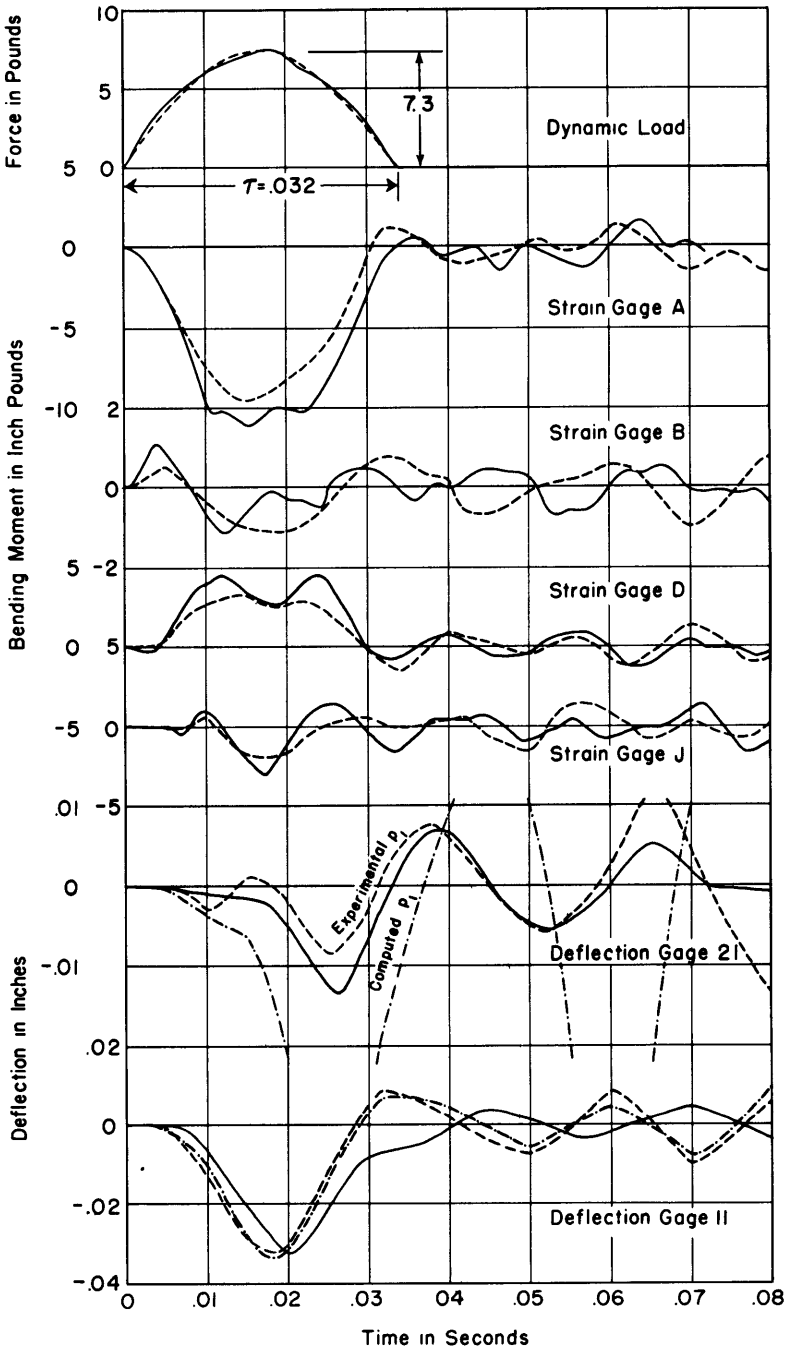

Figure 18 - Comparison of Experimental and Theoretical Response of Ring for k = 6.8 and τ = 0.032

Solid lines indicate experimental results.

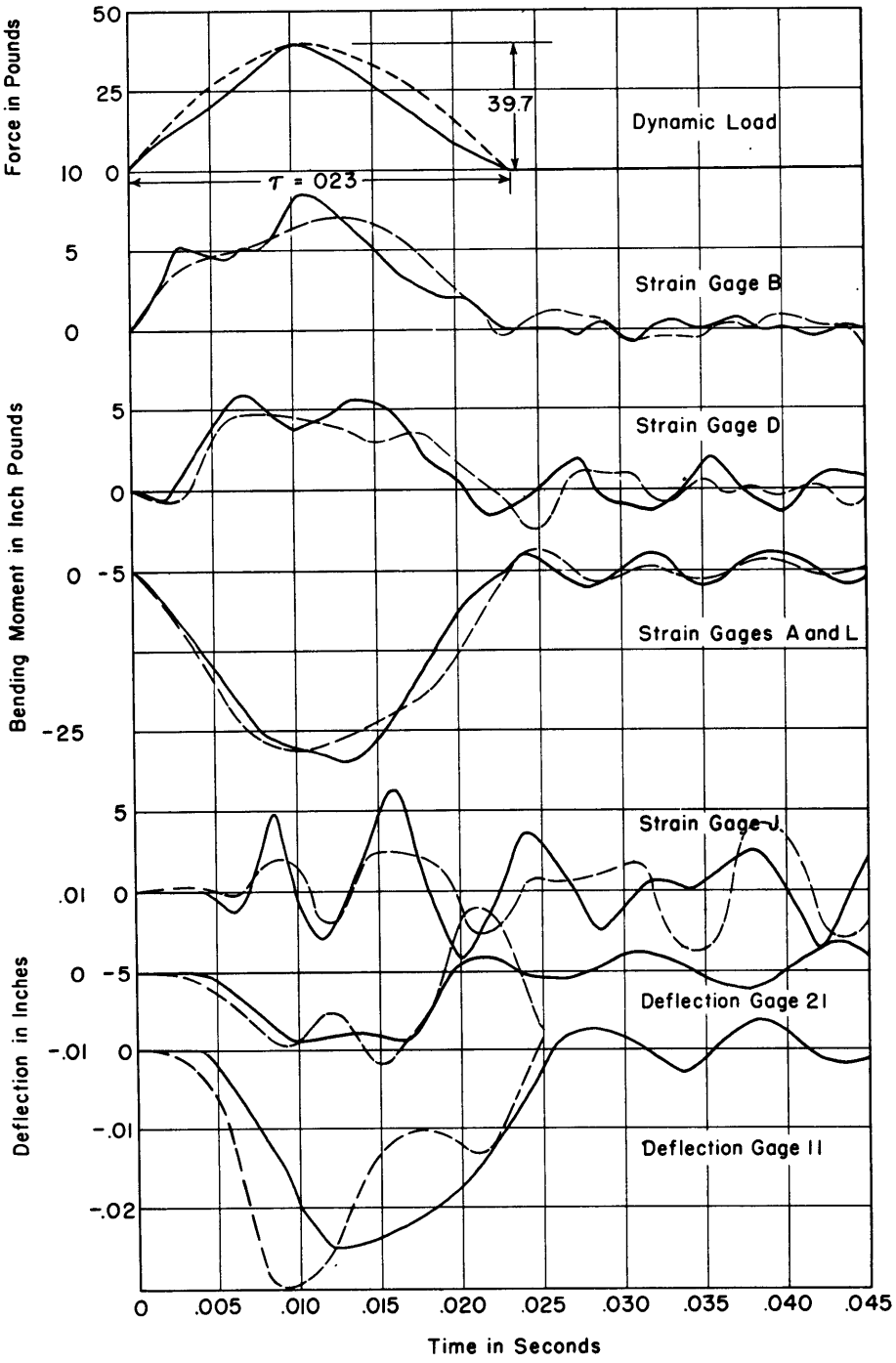

Figure 19 - Comparison of Experimental and Theoretical Response of Ring for $k = 31.6$ and $\tau = 0.023$

Solid lines indicate experimental results.

H. DISCUSSION OF AGREEMENT BETWEEN OBSERVED AND THEORETICAL RESPONSE FOR TRANSIENT LOAD

When the observed response is compared with the theoretical response, it is to be remembered that experimental errors exist in the measurements of response and of loading, and in the stiffness of elastic support; furthermore, the theoretical response as plotted includes only the first seven or eight terms of an infinite series solution, and so is incomplete.

In view of these possible sources of discrepancies, the agreement is all the more reassuring.

These results have additional significance in that the simplifying assumptions made in the course of deriving the theory are proved to have had negligible effects on the response. It will be recalled that these assumptions and restrictions were: (a) Uniform elastic radial support which exerts only radial forces in response to radial displacements; (b) inextensional vibration; (c) negligible effects of rotatory inertia; (d) negligible effects of shearing force; (e) negligible effects of damping; (f) assumptions of a thin ring.

It is known that the experimental apparatus exercised but little damping on the ring because of the observed persistence of response of even high-frequency components long after the end of the excitation. The agreement between observed and computed frequencies of vibration demonstrated the insignificance of extensional vibration and of the effects of shear and rotatory inertia. The deficiency of the apparatus, however, in providing pure elastic radial support, in contradiction to the assumptions made in the theory, produced as its only perceptible effect a change in response in terms of radial displacements; this effect incidentally can be rationally corrected if the frequency of rigid-body translatory motion is computed from elementary considerations.

I. DISCUSSION OF RANGE OF PARAMETERS EXPLORED EXPERIMENTALLY

It was not practicable to perform tests with more than one size of ring, so that the parameters which depend upon ring geometry were not varied. It may then be considered that experimental validation has been obtained only for the case of a thin ring where $\frac{EI}{r^4}$ is small. If $\frac{EI}{r^4}$ becomes large, that is, if the depth of the ring is very great compared with the diameter, its stiffness increases to such an extent that it is quite likely that shearing effects assume some importance. In fact, it is known from other experiments that where the depth of section is great compared to the length, the frequencies of free vibration and response to transient loading will depend upon such shearing effects. Most significant would be the reduction in frequency of

vibration of the higher modes from that which would be computed for flexural vibration. A similar effect would be expected in this case for the ring; and it is not known from this analysis for what range of $\frac{EI}{r^4}$ the theory becomes inapplicable. That is, it has not been determined where the threshold of importance of shearing effect may lie.

The values of P and τ which define the pulse were varied over a limited range. If, however, the stresses developed are within the elastic limit, no restriction exists on intensity of loading P. As for the duration, confirmation was obtained with static loading so that no upper limit exists to τ; the lower limit will undoubtedly arise when durations of loading are so short that longitudinal waves of significant amplitudes are generated.

5. SUMMARY AND CONCLUSIONS

A. RESTATEMENT OF IMPORTANT EQUATIONS OF RESPONSE

Equations have been derived for radial displacement and bending moment in a circular ring having elastic radial support and subjected to either steady-state forced vibration or transient loading. These equations are in the form of infinite series given by Equations [34] and [35] for steady-state forced vibration and for the period of action of a half-sine pulse, and by Equations [41] and [42] for free vibration subsequent to a transient pulse. Solutions for the limiting case of static loading are given by Equations [43] and [44].

The frequency of free vibration including the effect of elastic radial support is given by Equation [15]. It was found that the addition of moderate elastic tangential support influences only the radial displacements and the frequency of rigid-body translation. Frequencies including this effect are given by Equation [15a].

B. EXPERIMENTAL INVESTIGATION

An experiment has been performed with a ring 24 in. in diameter having a cross section 1 in. by 1/8 in. supported elastically with 38 coil springs and subjected to a radial impulse having as its time history a half-sine pulse. The intensity and duration of pulse as well as the stiffness of the springs were varied, and observations were made of the response.

For the purpose of applying an analytically described transient load to the ring, a special pulse generator was developed and put into operation. Also, a dynamometer was developed for measuring the dynamic load.

Measurements were made of frequencies of free vibration and of bending moments and radial displacements produced by transient loading. The experimental errors present in the test were carefully investigated and, on the basis of consistency of results, were on the order of 5 percent.

C. AGREEMENT BETWEEN THEORY AND EXPERIMENT

It was observed that with steady-state forced vibrations, the frequencies of the various modes agreed with values computed by the theory within a few percent, even up to the seventh flexural mode. Further, the observed response to a half sine pulse in terms of time functions of displacements and bending moments agreed reasonably well with theoretical values.

D. CONCLUSIONS

It is therefore concluded that the experimental procedures employed in this test were satisfactory and that the mathematical analysis for an elastically supported ring is applicable for a ring having thickness and depth small compared with the diameter.

ACKNOWLEDGMENT

The author wishes to express his appreciation to Capt. R.A. Hinners, USN, Comdr. T.H. Frost, USNR, and Dr. William R. Osgood for their support and encouragement of this basic research investigation, and to Dr. William H. Hoppmann, II, of The Johns Hopkins University for his constructive comments regarding development of the theoretical analysis.

The author also wishes to acknowledge the cooperation and assistance of Miss Margaret E. Duke, R.L. Hughes, and V.L. Mildenberg with the computations and conduct of the experiment.

APPENDIX 1

APPLICATIONS

A discussion is set forth in this appendix of the engineering procedures required to determine the maximum response for strength design.

A. GRAPHICAL SOLUTION OF FREQUENCY EQUATION

As a first step, there has been derived a graphical solution of the frequency equation [15]. From this chart, Figure 20, it is possible to relate quickly the three important parameters which govern frequency for the various modes of vibration. Information regarding frequency may also be extracted for solution of the equations which define response to dynamic loading. When employing this chart, if the $\frac{EI}{r^4}$ value is less than 1, multiply both its value and that for k by 100, solve, and divide the frequency p_i obtained from the right-hand scale by 10.

B. STRENGTH CALCULATION OF RINGS

With reference to Equations [41] and [42], it will be observed that $\cos \frac{p_i \tau}{2}$ varies between +1 and -1 and is critically dependent on the value of τ, that is, the duration of the pulse. In most actual cases, this value is not explicitly known. Thus, when making engineering calculations, it would be advantageous to employ the maximum numerical value of +1 or -1 so as to obtain a result known to be on the side of safety.

When the transient load is considered as concentrated at $\theta = 0$, it is important to observe that the coefficient $\cos i\theta$ in calculations for response both during and after the pulse is always +1. Thus the maximum intensity of displacement and bending moment occurs at the point of application of load, and further examination of response elsewhere around the ring may be unnecessary.

The instant at which such response is a maximum may not be so easily derived; and, as a consequence, a plot of time history may be required of all modes of significant amplitudes. The number of modes, of course, depends on the rate of convergence which, in turn, is a function of the duration of the pulse. Nevertheless, it will be noted that the pattern of the response at the point of application of load corresponds exactly to the shape of the forcing function; that is, for a half-sine pulse, the envelope for all modes will also be a half-sine pulse. Subsequent free vibrations again composed of numerous components may be more irregular in shape. Of course, if the exciting pulse is short, the subsequent free vibrations will greatly exceed response during the action of the load.

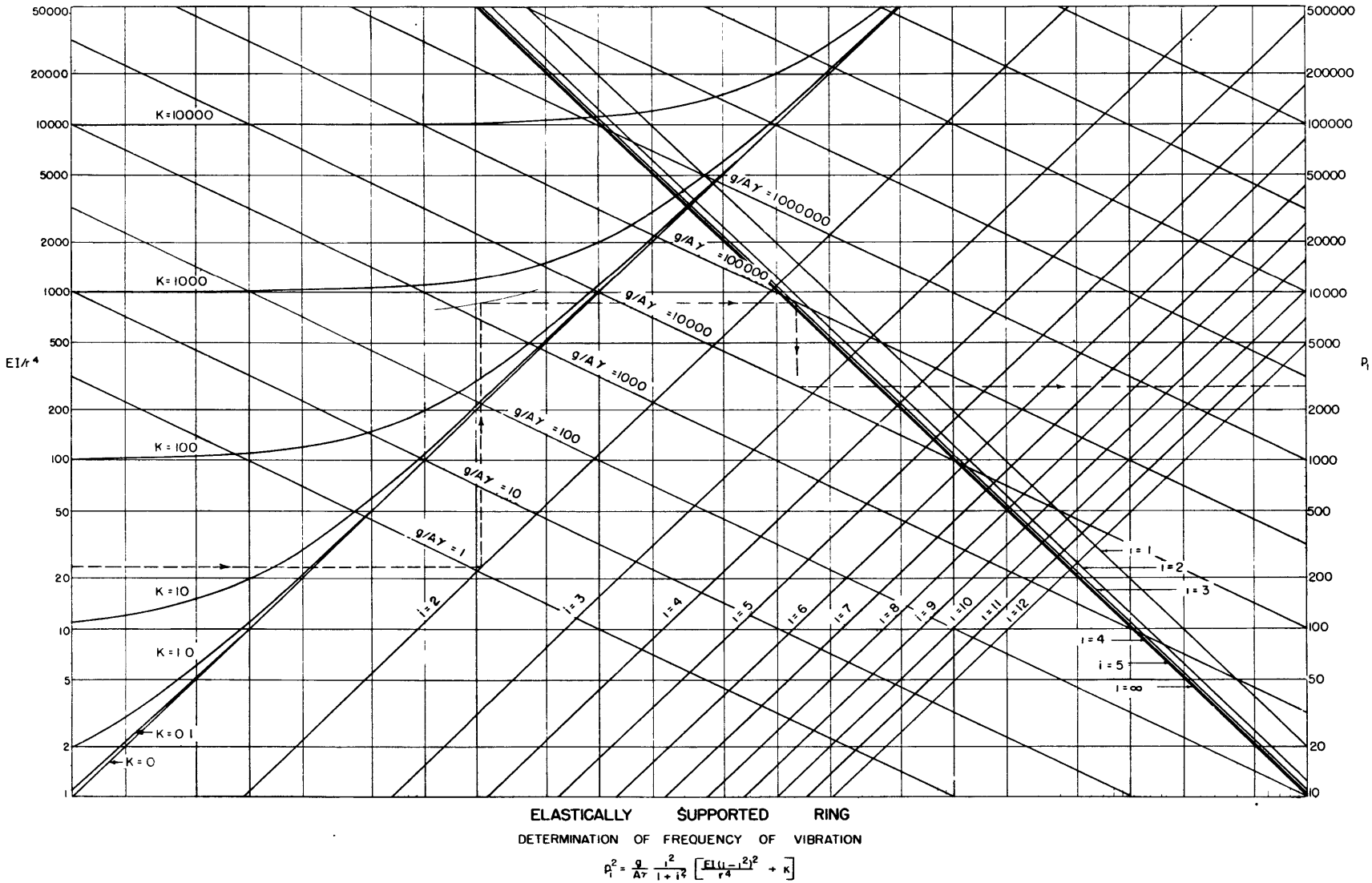

Figure 20 - Nomogram of Frequency Equation for Elastically Supported Ring

A sample solution for p_i is shown by the broken line. For values of EI/r^4 less than 1, multiply by a factor of 100, also multiply the value of k by 100, and divide the solution of p_i by 10.

C. POSSIBLE LIMITATIONS OF THEORY DUE TO SIMPLIFYING ASSUMPTIONS

There is such a variety of applications for this theory of an elastically supported ring—to wire wheels, frames of motors and turbines, aircraft fuselages, etc.—that it would not be possible to examine fully all possible departures of a real structure from the idealized ring treated here. The departure most to be expected is an elastic support that acts with tangential as well as radial displacements, but as shown for the specimen under test, this constraint may not seriously influence bending moments.

Other limitations may arise if the ring were so stiff that shearing effects might be significant so that a limitation on the ratio of ring depth to diameter is the only definite restriction imposed on the theory.

APPENDIX 2

DETAILS OF EXPERIMENTAL APPARATUS AND TEST INSTRUMENTATION

A. INTRODUCTION

Additional information concerning the experimental analysis of the elastically supported ring is provided here for possible use as a guide in the planning and conduct of other similar tests of structural models, and for a detailed evaluation of the worth of the results presented in the body of the report. The means for applying and measuring load proved to be satisfactory and bears further consideration and investigation as a technique applicable to dynamic testing of structural models.

B. DESCRIPTION OF THE RING

When selecting the size of the ring, consideration was given first to the relationship between the frequencies of flexural vibration and the important parameters of ring diameter, ring cross section, and stiffness of elastic support. Since it was considered likely that damping in the system would be minimized, excitation of flexural modes as high as the eighth order could be expected; then a limit of 450 cps was placed on this estimated eighth-order frequency based on the response of a string oscillograph which was believed in advance to be the best instrument for simultaneously recording the time history of several variables. A trial size of ring was selected with circular cross section, but the circular section was discarded in favor of the rectangular section to simplify attachment of the ring to the elastic support and mounting of strain gages. As a result of these considerations, a ring was

chosen with an outside diameter of 24 in. and a rectangular cross section 1 in. wide and 0.125 in. deep.

Although an accurately machined ring was desired for the test, it was decided for reasons of economy to manufacture the ring by rolling a hoop out of flat bar stock and welding together the two ends. The diameter was within 1/16 in. of the required 24 in. The material employed was cold-rolled steel with a modulus of elasticity E of 29.2×10^6 lb/in.^{2}

C. DESCRIPTION OF ELASTIC SUPPORT

In the process of selecting dimensions of the ring, consideration was also given to the practical ranges of stiffness of an elastic-support system such that the effect of variation of this parameter on the frequency of vibration could be readily measured. It was intended to have one stiffness of elastic support sufficient to raise the frequency corresponding to the fundamental mode of flexural vibration of the unconstrained ring by a factor of 2, and a second stiffness to raise that frequency by a factor of 4. With the 24-in. ring, the two values of modulus k which satisfy this requirement were computed from Equation [15] to be 6.33 lb/in./in. and 31.6 lb/in./in., respectively.

It was decided to employ mechanical springs for the elastic support and, although these would not possess the continuous character of the idealized support, it was believed that continuity would be very well approximated by spacing the springs around the periphery at 2-in. intervals.* To obtain an elastic support of k = 6.33 and k = 31.6 on a ring 1-in. wide, the springs with 2-in. spacing should have constants of 12.66 and 63.2 lb/in. respectively.

For this purpose, consideration was given first to a system of flat-leaf springs. A problem arose, however, as to the dimensions of leaf springs which would have the desired properties of stiffness and range of deflection, and at the same time would possess an inherent natural frequency of 1200 cps—that is at least three times greater than the highest frequency of vibration of the ring that was desired to be observed. This latter stipulation was introduced to guarantee that the elastic support itself would not absorb energy from or alter dynamical behavior of the vibrating ring.

---

*Consideration was given to the use of a thin shell as an elastic support because of its continuity; but because the plating would be so intimately associated with the ring, it would not be possible to describe the explicit cross-sectional properties of the ring which were required to be known for the analysis of its dynamical behavior.

The parameters for leaf springs of width, thickness, length, elastic modulus, etc., are related as follows:

$$f = \frac{3.52}{2\pi}\sqrt{\frac{Eh^2g}{12\gamma l^4}} \qquad [52a]$$

$$\Delta = \frac{Pl^3}{3EI} = \frac{4Pl^3}{Ebh^3} \qquad [52b]$$

$$\sigma = \frac{Plh}{2I} = \frac{6Pl}{bh^2} \qquad [52c]$$

$$\text{Spring constant} = P/\Delta \qquad [52d]$$

$$f = \frac{0.6\sigma}{\Delta\sqrt{E\gamma}} \qquad [53]*$$

where l, b, h are the length, width, and thickness of spring in inches,
f is the natural frequency in cycles per second,
σ is the allowable stress in pounds per square inch, and
Δ is the desired deflection in inches.

It was found that no leaf springs could be found compatible with these relationships which would provide the desired characteristics for the springs with k = 6.33.

Resort was then made to coil springs as a means of elastically supporting the ring, in the arrangement as shown in Figures 7 and 8 on pages 24 and 25. The weight of the ring is supported by the lateral stiffness of the springs.

Although not previously stipulated, it was tacitly assumed in the theory that elastic support to the ring is furnished with radial displacements either toward or away from the center. This effect could be achieved when using coil springs simply by installing them in an initially extended state. So that elastic support would be linear within the expected range of deformation, the amount of initial extension was specified to be 20 percent in excess of the maximum anticipated deflection of the ring (estimated for k = 6.33 to be 0.3 in.). This required, in the course of the spring design, that the spring be capable of sustaining a total extension of 2.2 times the estimated maximum deflection. As before, the springs were also required to possess a natural frequency in excess of 1200 cps. The dimensions of springs with the desired

*Note that this equation excludes all parameters of size.

characteristics were computed from standard criteria[22] and are given, together with a diagram showing pertinent dimensions, in Figure 21.

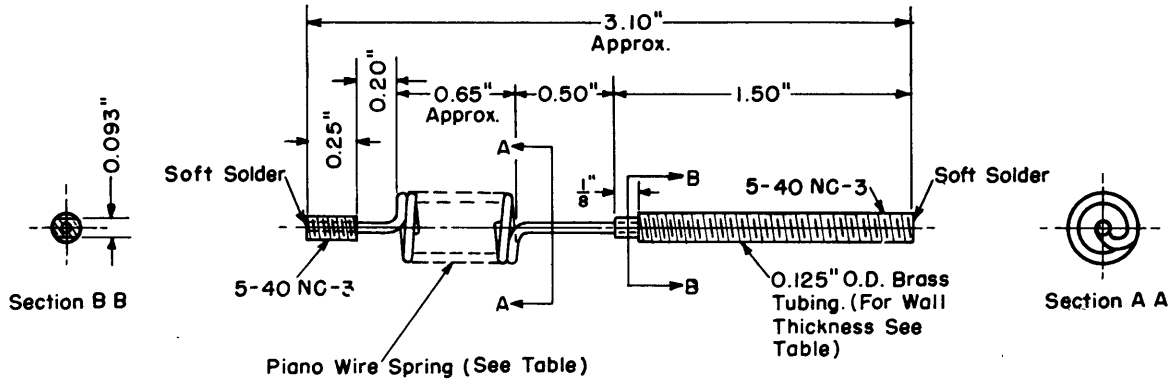

	Spring Pc. 1	Spring Pc. 2
Spring Constant - lb/in. Deflection	12.66 ± 5 %	63.2 ± 5 %
Diameter of Wire	0.043	0.058
Mean Diameter of Spring	0.30	0.30
No. of Active Coils	15	10
Load Applied - pounds	12.66	30.0
Wall Thickness of Tubing for Ends	0.035	0.032

Figure 21 - Detailed Construction of Coil Springs

Brass tubing was soldered at each end of the spring and threaded for attachment to the ring and to the hub on which the ring is mounted. Dimensions of the two different size springs are given in the table.

Although only 38 springs in each of the two sizes were required for this installation, it was decided to manufacture 50 so that, should the spring constants not be uniform, the best out of 50 could be culled.

All springs were calibrated statically with dead weights using the apparatus shown in Figure 22; the axial extension was measured with a dial indicator. A plot of the load versus extension is shown for a typical spring of k = 6.33 size in Figure 23. As will be noted, these springs demonstrated a nonlinearity at the initial loads. This nonlinearity was attributed to initial pressure between the coils of the spring, which was relieved upon application of small loads. Because it was planned to stretch all springs initially when installed, so as to provide elastic support with inward as well as outward motion, this initial nonlinearity was not cause for rejection. It was thus possible to define the spring constant in terms of the force-versus-extension relationship which was observed to be linear after the initial extension.

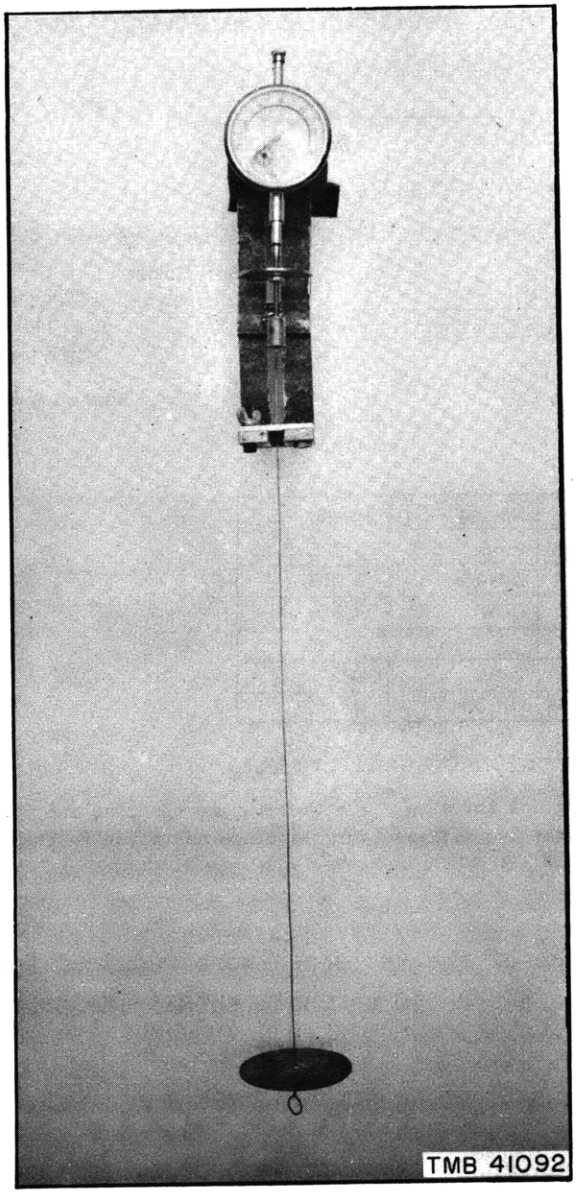

Figure 22 - Device for Calibrating Coil Springs Which Elastically Support the Ring

The stiffness factor of all springs was checked with this device, which indicates extension during deadweight loading.

It will also be noted that the calibration did not agree with the specified spring constant within the allowed deviation of 5 percent.* The average spring constant for the more flexible of the two sets of springs was 13.6 lb/in. as compared with the 12.66 lb/in. desired; and after this discrepancy was observed, the experimentally determined value for the spring constant was employed in both theoretical and experimental work described in the report. The modulus of support corresponding to this spring constant was 6.8 lb/in./in. instead of the desired 6.33. The stiffer springs of constant 63.2 lb/in. to produce a $k = 31.6$ were found to be satisfactory within the 5 percent allowable deviation.

Although the dynamical behavior of the ring is not a function of the initial tension in the springs, apart from the requirement that the tension be sufficient to provide linear elastic support over the full range of deflection, equal tension in all the springs was nevertheless desired to guarantee the circular shape of the ring. To check the initial extension, a device was manufactured as shown in Figure 24. This device consisted simply of an anvil-shaped gage with electrical

*The failure of the $k = 6.33$-size springs to agree with the specified spring constant could not be explained even by the spring manufacturer who employed the same criteria for design as had the author. It would thus appear that the criteria are not sufficiently exact, at least in this range of spring size.

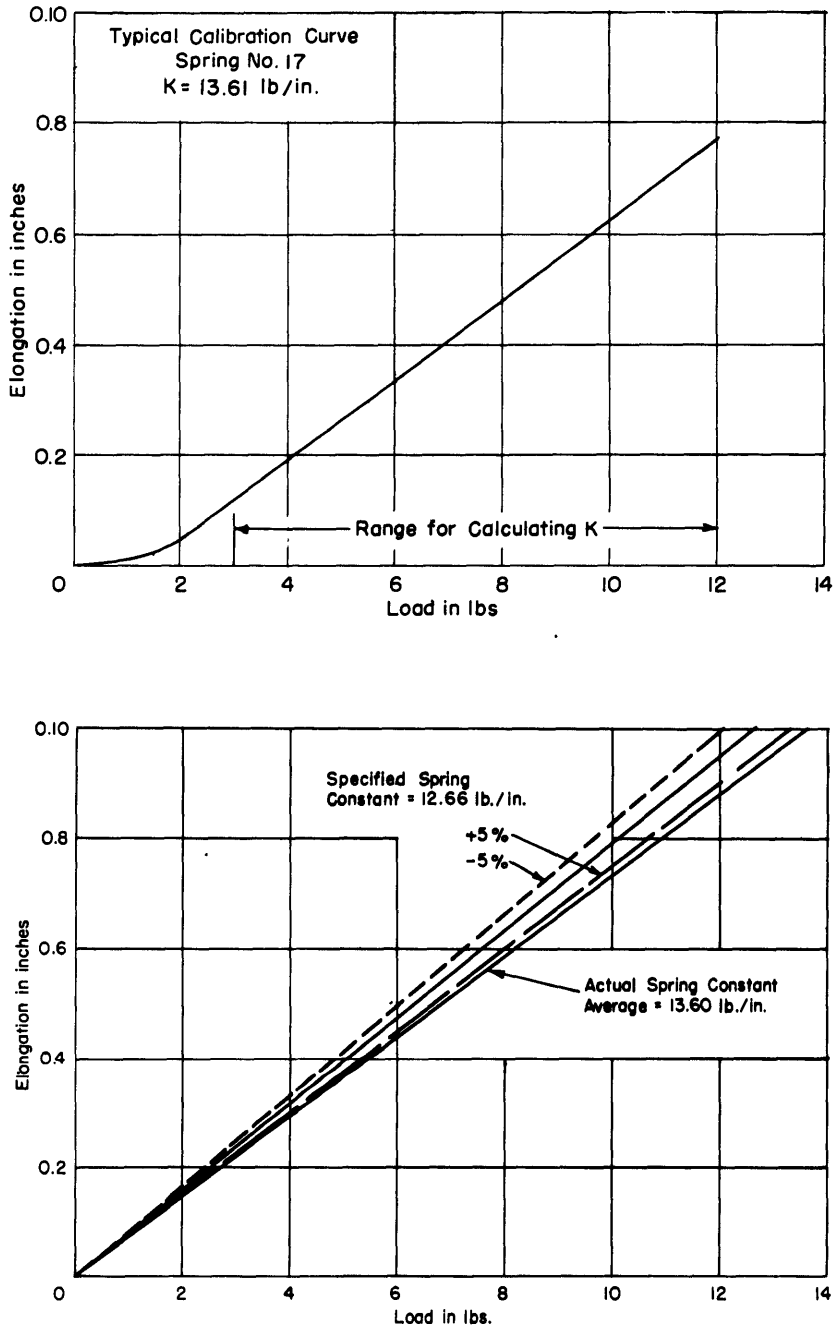

Figure 23 - Spring Calibration

The springs showed linear extension after the coils were opened, and since all springs were to be prestressed when installed, they would always operate within the linear range. The spring constant was computed from the straight line through the plotted points.

The spring constant observed for the more flexible set of springs differed from the specified value of 12.66 lb/in.; the observed value of 13.60 lb/in. produced a modulus of elastic support k = 6.8 which was employed in numerical computations.

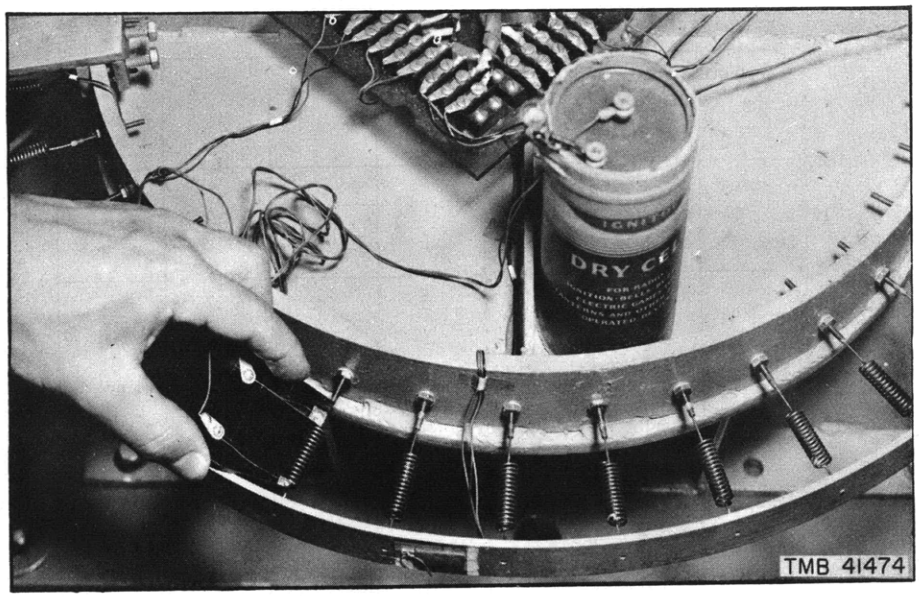

Figure 24 - Gage for Establishing Uniformity of Spring Tension

To maintain the circular shape of the ring, initial tension of springs was required to be uniform. This was accomplished with a gage which had electrical contacts properly spaced so that an indicating circuit would be closed when the spring was distended the correct amount.

contacts on the two opposite arms. These contacts were connected in a series electrical circuit with a dry cell and flashlight bulb, and the anvil was held during adjustment of the spring in such a position that, when the spring had been properly tensed, the circuit was closed and the bulb illuminated.

The initial tension in all springs was 4.25 lb, or 2.12 lb per in. of circumference. The buckling load for the ring was computed[3] from the expression $q_{cr} = \frac{3EI}{r^3}$ to be 8.5 lb/in.

D. DESIGN OF PULSE GENERATOR FOR APPLYING TRANSIENT LOADS

Because the major development of the theory is for the case of transient loading, a generator was required to apply to the ring a controlled radial impulse with a pure half-sine characteristic. A system for measuring the applied load was also required.

Heretofore, the most frequently employed means of loading an elastic structure has been through impact of a small sphere dropped onto the test specimen from a controlled height. By application of Hertz's contact theory,[18] as extended by Lee, Hoppmann, et al[14, 15, 23, 24, 25] it is possible to estimate the duration, intensity, and "shape" of the applied load. A limit to the validity of the theory obviously occurs when the specimen being struck has diminutive mass or stiffness compared with that of the striking sphere. Also

implicit in this theory are short durations of contact compared with the fundamental period of ring vibration. Since longer durations of contact were desired for this investigation, it was considered advisable to explore other means of applying load.

1. Guided Ballistic Pendulum

It was at first decided to employ for this test a facility which had been developed at the Taylor Model Basin for the purpose of applying controlled dynamic loads to rigid bodies. As shown in Figure 25, this device is a ballistic pendulum consisting of a mass suspended on wires which was allowed to strike a guided car. The car, after being struck by the pendulum, moves at constant velocity and, after a short travel, strikes the test specimen. Interposed mechanically between the car and specimen is a spring system whose stiffness could be adjusted if desired. Theoretically, and as observed experimentally, this ballistic pendulum, when striking a rigid body, would develop an almost pure half-sine pulse of a duration and intensity which depended upon the parameters of spring constant, mass of the car, mass of the pendulum, and stroke of the pendulum. Smoothness of pulse was assured by use of a 1/2-in. rubber pad at the point of impact.

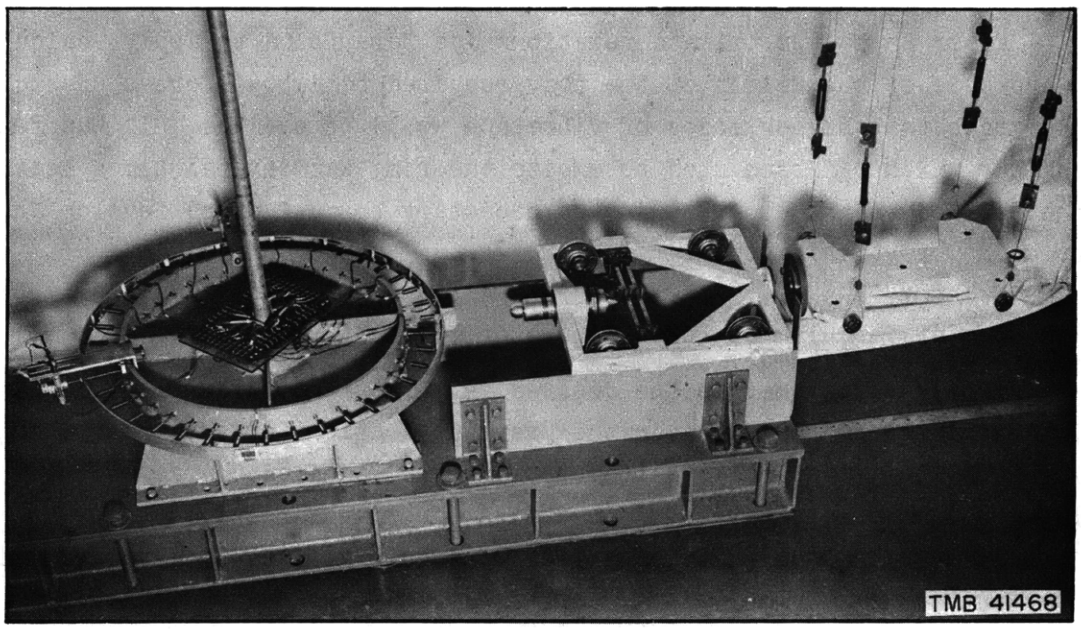

Figure 25 - Arrangement for Dynamic Loading of Ring by Means of Guided Ballistic Pendulum

A radial impulse is delivered to the ring by means of a guided car which is set in motion at constant velocity by impact from a pendulum dropped through a controlled stroke. The time history of force is measured with the dynamometer mounted at the leading edge of the car.

When this facility was used to excite the ring, it was found that the duration and intensity of force was governed not only by the characteristics of the striking system but also by the flexibility of the test specimen. This flexibility was found to be defined simply on the basis of static deflection of the ring at the point of contact, per unit load. The duration of load was found to be determined by the approximation to a single-degree-of-freedom system as:

$$\tau = \pi \sqrt{\frac{u_s' (W_r + W_p)}{g}} \qquad [48]$$

where τ is the duration of the pulse,

u_s' is the static deflection per unit load at the point of application,

W_r is the lumped weight of the ring and spring system, and

W_p is the weight of the body striking the ring.

By considerations of momentum of the system,* the intensity of force imposed on the ring by a free body traveling at constant velocity $\bar{v}$ is

$$P = \frac{u_{max}}{u_s'} = \frac{2 W_p \sqrt{W_p + W_r}}{(2 W_p + W_r)\sqrt{u_s' g}} \bar{v} \qquad [49]$$

After these approximate relationships were found to apply, calculations were made of the weight of the body required to impose forces of such short duration that higher modes of vibration would be excited. It was found that the car which had been used to excite the ring was several times heavier than the desired weight, so that it was necessary to design and develop an alternate means of striking the ring.

2. Design of Pendulum as Pulse Generator

In order to generate the desired intensity and duration of loading pulse, the criteria established in the previous section for a mass striking the ring were applied as follows to determine the required characteristics of a pendulum which would be arranged to strike the ring directly.

The terminal velocity of a free pendulum, at impact, is approximately

$$\bar{v} = \sqrt{\frac{g}{L}}\, d \qquad [54]$$

---

*A similar approximate analysis based on considerations of energy rather than on momentum was made by Timoshenko for impact on beams where the mass of the beam was small compared with that of the striking body.

where L is the length of the pendulum and d is the stroke (assuming $d \ll L$). Thus the applied load can be computed as

$$P = \frac{2 W_p \sqrt{W_p + W_r}}{2 W_p + W_r} \frac{d}{\sqrt{u_s' L}} \qquad [55]$$

These results were verified experimentally as shown in Table 4.

TABLE 4

Comparison of Observed Characteristics of Transient Loading with Those Computed by the Derived Criteria

Modulus of Elastic Foundation k lb/in./in.	Computed Static Deflection u_s' in./lb	Weight of Pendulum W_p lb	Impact Pad during Test	Stroke of Pendulum d in.	Computed Duration τ sec	Observed Duration τ sec	Computed Load P lb	Observed Load P lb
6.8	0.0090	5.2	Yes	—	0.043	0.047	—	—
6.8	0.0090	2.2	Yes	6	0.034	0.032	6.5	7.3
31.6	0.0021	2.2	No	—	0.0166	0.016	—	—
31.6	0.0021	2.2	Yes	18	0.016	0.023	41.3	39.7
31.6	0.0021	1.2 ball	No	—	0.014	0.012	—	—

For the tests, a simple brass bar was selected as the body for the pendulum, as shown in Figures 7, 8 and 26. It was 2 in. in diameter, of length as desired to make up the necessary mass, and was suspended with phosphor-bronze wire from an arm which was attached to a pipe vertically supported in the base. A threaded hole was provided at one end of the brass bar to receive the load dynamometer.*

As the result of experience derived from tests with the guided pendulum, a rubber impact pad was attached to the ring at the point of contact to reduce high-frequency fluctuations of load. With the dynamometer in place and the supporting wires of the pendulum adjusted so that the impact head of the dynamometer was at incipient contact with the impact pad with the dynamometer

*A steel ball 2 in. in diameter was also used during a few tests to strike the ring to provide a simple check on time of contact; see Figure 29 on page 63. Durations of contact were determined electrically and were found to exceed by a large factor the duration computed by Hertz's theory for two spheres, one assumed very large; the criteria advanced in the foregoing were found applicable.

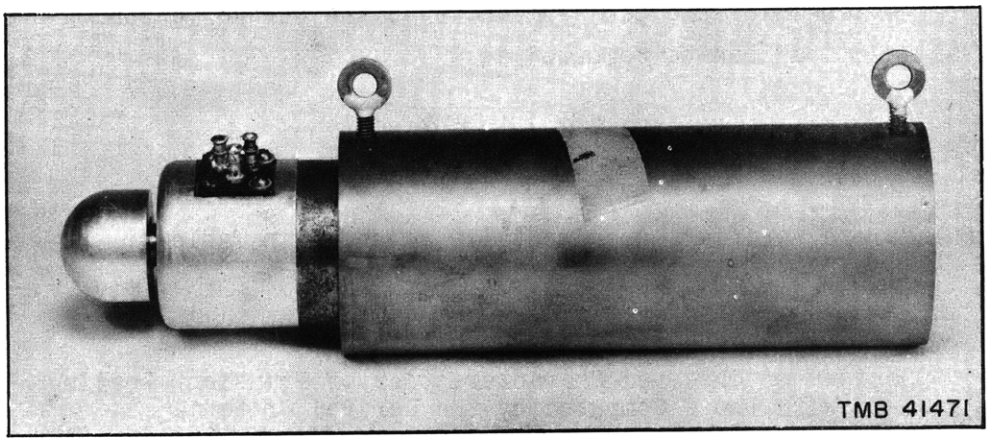

Figure 26 - Pendulum with Dynamometer

Since it was found that duration of load was a function of the mass of pendulum, two different size pendulums were employed to develop pulses of different durations. Both were of brass, 2 in. in diameter, and of a length selected to provide the desired mass. One end of each pendulum was machined to receive the threaded shank of the dynamometer.

at rest, excitation of the ring was provided simply by drawing back the pendulum by hand through a specified stroke and releasing it, catching it again by hand on the rebound. The amount of rebound, incidentally, was approximately 60 to 80 percent of the stroke.

This means of exciting the ring was found to be satisfactory in so far as it produced a half-sine pulse of controlled duration and intensity.

E. THE LOAD DYNAMOMETER

For the study of mechanical properties of materials under rapid loading where it is necessary to measure the time history of load, there have been developed in recent years several means for directly and accurately measuring impulsive loads. Such dynamometers have been devised with a solid-steel bar on which were bonded wire- or carbon-resistance gages which would follow the axial deformation of the bar. The change in resistance of the gages was detected by a suitable electrical system and registered as desired on an oscilloscope.

Similar devices which employed wire-resistance strain gages have been recently developed at the University of California[26] and also at the Massachusetts Institute of Technology,[27] but none of the information concerning their design was available to the author at the beginning of studies of a dynamometer for this particular application. An independent development of a dynamometer was thus undertaken to meet the following requirements. The maximum forces to be applied to the elastically supported ring were estimated to

be on the order of 100 lb. Further, the duration of loading was expected to be as short as 5 milliseconds. There was thus fundamentally required a dynamometer system which had sufficient sensitivity to measure forces on the order of 1/10 of the maximum anticipated, that is about 10 lb, and which at the same time possessed a natural frequency sufficiently high that response of the instrument could be relied upon for brief transient loads.

Additional design requirements were stipulated as follows:

1. Calibration of dynamometer should be simple and should not require elaborate equipment.

2. Once determined, the instrument calibration should remain independent of age and extremes of meteorological conditions and should not be disrupted by handling.

3. The response of the device should be free of spurious indications when exposed to shock and vibration and to normal variations of temperature of the ambient atmosphere.

4. Superposed instrument errors should be less than 2 percent of the maximum force being measured.

5. Provision should be made for recording at a station remote from the point of instrument installation.

6. Manufacture, assembly, installation, and operation should be simple, and the dynamometers should be compact and durable and have the finished appearance of a commercial product.

With due consideration for the availability of auxiliary electrical or electronic equipment which was known to be required for use with any dynamometer, and from successful prior applications of wire-resistance strain gages, it was decided that the dynamometer should comprise a simple mechanical form on which strain gages would be mounted to detect elastic deformations of the mechanical body under load.

Such geometric forms as rings, bars, frames, and tubes could be employed, but of these only an axially loaded tube showed promise of having a sufficiently elevated natural frequency that high-speed phenomena could be satisfactorily measured. Essentially, then, the dynamometer was designed as a short column of hollow circular cross section on which strain gages were mounted to measure deformations under axial load.

To provide maximum sensitivity, the cross-sectional area of the column was reduced to a minimum consistent with requirements of elastic stability, ease of manufacture, and space for mounting the strain gages. The tube finally adopted had an outside diameter of 1/2 in. and a minimum wall thickness of

1/100 in., and was made as short as practicable to guarantee high natural frequency of axial vibration. A schematic diagram of the instrument is shown in Figure 9.

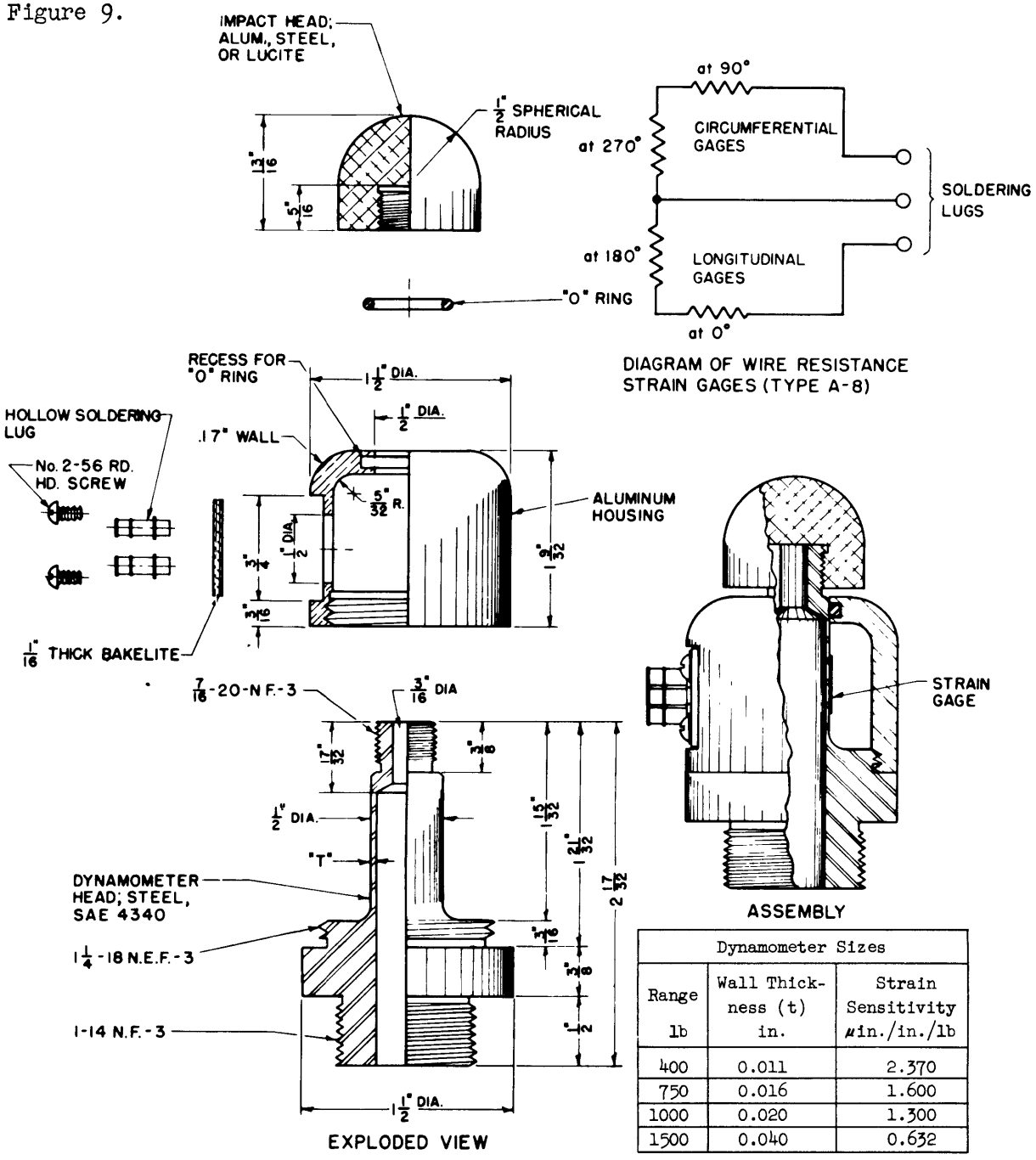

Dynamometer Sizes		
Range lb	Wall Thickness (t) in.	Strain Sensitivity μin./in./lb
400	0.011	2.370
750	0.016	1.600
1000	0.020	1.300
1500	0.040	0.632

Figure 9 - Construction Details of the Load Dynamometer

The force of impact was measured with strain gages mounted on a hollow tube which would be axially loaded. Orientation of gages was selected to minimize sensitivity to bending and torsion of the tube and to temperature effects.

The instrument sensitivity depends on wall thickness as shown in the table, and the natural frequency depends on the length. For this instrument it was in excess of 50,000 cps.

With the hollow tube, there is integrally provided a heavy base with threaded shank for mounting, and also a threaded projection to engage an aluminum housing which is fitted around the tube to protect the strain elements from mechanical damage. The other end of the tube is threaded to receive an interchangeable impact head which can easily be removed if damaged or permanently deformed.

Four strain gages were mounted on the tube, two longitudinally and two circumferentially. When electrically connected as shown in Figure 9, this combination of gages automatically compensates for changes in temperature and for any bending of the tube which may inadvertently be caused by eccentricity of axial loading; either of these effects would reduce precision of the instrument. Further, this combination of gages provides a strain sensitivity approximately 30 percent greater than the axial strain developed in the tube, as the result of the algebraic sum of the axial strains and the circumferential strains which are produced by the Poisson effect.

The strain gages were applied carefully in accordance with the techniques in use at the Taylor Model Basin and, after waterproofing, were electrically connected to the soldering lugs mounted on the housing that protects the strain elements. Complete water-tightness of this compartment was assured by the "O"-ring located at the top of the housing, which, while preventing entrance of moisture, was found from tests not to interfere with the transmission of load from the head of the sensitive tube to the shank. That is, virtually no friction was introduced at this moisture seal.

Calibration of the dynamometer was performed statically in a Universal testing machine of 30,000-lb capacity, using the 3,000-lb range. The electrical output was measured with a Baldwin-Southwark Type-K strain indicator* as shown in Figure 27; a typical calibration curve is shown in Figure 28.

The dynamometer, designated as a Number 1-A elsewhere in the report, was employed in all important tests. From calibrations performed on 27 July 1949, its sensitivity was found to be 0.422 lb/μin./in. (2.37 μin./in./lb). A later calibration performed upon conclusion of the tests on 18 October 1949 checked this value exactly.

Other tests were performed to determine if any spurious indications would develop due to eccentricities of loading, and it was found that such sensitivity to extraneous forces was negligible. No tests were conducted to determine the sensitivity to changes in temperature, but it was known from elaborate studies of an elastic-tube pressure gage[28] (which is similar in

*Indicator Number D-58144 was used with gage factor setting of 2.00.

Figure 27 - Load Dynamometer and Indicator

Forces applied to the ring were measured with the dynamometer. The strain indicator was employed to measure electrical output of the dynamometer during static calibration.

construction to this dynamometer) that, with the combination of strain gages as provided, adequate temperature compensation is achieved over a range of zero to 140° F.

Inasmuch as the dynamometer employed in all the tests had a strain sensitivity of only 2.37 μ in./in. per lb of load, with loads of about 10 lb, the output in terms of strain units was approximately 25 or 30 μ in./in. This is an extremely small strain, and it was only by use of sensitive electronic equipment with high amplification that it was possible to record the signal. The amplifier employed with the dynamometer was a TMB Type-1A strain indicator[19] which had a linear frequency response from 0 to 200 cps. This frequency range was ample here where the duration of load never was less than 15 millisec; but had the duration been much shorter, some other amplifying and recording system would have been required to register without distortion

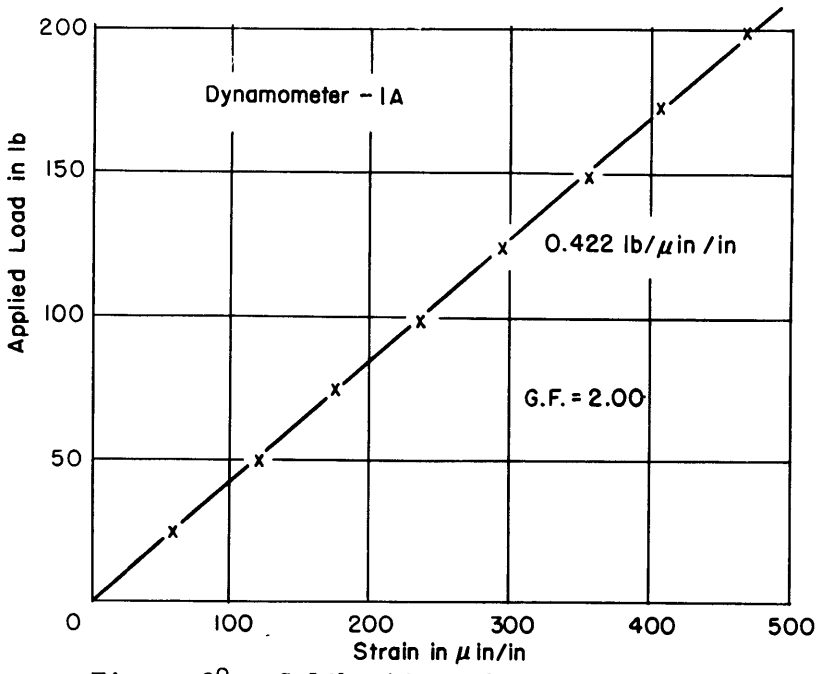

Figure 28 - Calibration of Dynamometer

Response was found to be a linear function of applied load, either increasing or decreasing. Zero shift before and after loading was zero.

electrical signals produced by the gage. The dynamometer itself has such a high natural frequency that it may be used to measure forces lasting as short a time as 0.01 millisec.

Since the dynamometer was calibrated with a testing machine having a possible error of 1/2 percent, the absolute error of the dynamometer is of that order. However, with the use of auxiliary equipment other than that employed during calibration and with errors which result during recording, errors in load measurement may be as great as 5 percent. These errors are discussed in greater detail on page 66.

F. EXCITATION OF STEADY-STATE FORCED VIBRATIONS

When the dynamical tests were first performed, periodic oscillations of response were observed, and it was believed that the frequencies corresponding to the various modes of flexural vibration could be extracted from the records. After careful examination, however, it was found that no repetition of patterns occurred, at least sufficient to permit the determination of these frequencies with any high degree of accuracy. It was therefore decided to excite the ring with a steady-state forced vibration over a broad band of frequencies and to discover the natural frequencies by observation of resonance.

A heavy-duty dynamic loud-speaker element was employed to excite the ring. The light voice coil of the dynamic speaker, consisting of a fiber ring about 1 in. in diameter with a winding of approximately 10 turns of number 26 wire, was attached rigidly to the ring and brought into the field of an electromagnet energized by a 300-v d-c source. The voice coil was then driven by an a-c output from a Hewlett-Packard audio oscillator, Model 200-B. Since the oscillator was not a precision instrument, the exciting frequencies productive of resonance were determined accurately by recording the outputs of several strain and deflection gages simultaneously with a precise timing pulse. Incidentally, the excitation of resonance was easily detected from audible sounds from the vibrating ring, as well as by visual observation of the strain-gage signals.

G. INSTRUMENTATION TO MEASURE STRAIN AND DISPLACEMENTS

Bending moments were determined from circumferential strains, measured by wire-resistance gages; a comprehensive discussion of these instruments is given by Dobie and Isaac.[29] With the mechanical arrangement of ring and springs, it was feasible to mount strain gages only by interspersing them with the springs. Gages were mounted in this fashion on one-half of the ring, and additional gages were mounted on the other half of the ring to provide a check on results through symmetry of gage location with respect to the axis of loading. These gage locations are shown in Figure 10 on page 29; and angular positions are given explicitly in Table 3, page 22.

Strains, e, were converted to units of bending moment by the relationship $M = \frac{IeE}{2c} = 0.038\ e$ where the factor 1/2 was introduced to account for the doubled strain produced by two gages located on opposite sides of the ring and electrically connected together.

For the measurement of radial displacements of the ring, consideration was given to available instruments, such as a flexible cantilever on which were mounted wire-resistance strain gages, a photoelectrical meter, various types of condenser or reactance gages and particularly to a spring-type transducer developed by Dr. Wildhack at the National Bureau of Standards.[30] The apparatus adopted primarily on the basis of previous successful application was a transformer-type gage as manufactured by the Schaevitz Corporation.[20] It consists of a transformer having a primary energized with alternating current and two secondary coils wound on a hollow tube and differentially connected. A small steel core free to move in the tube produces an electrical output whose voltage is proportional to the motion of the core relative to the transformer. This output is also alternating current with a frequency the

same as that of the source of power to the transformer and an amplitude proportional to displacement regardless of the direction in which the core is moved relative to the null position.

Since phase reversal of the electrical output occurs with motion of the core in the two opposite directions, it is possible to introduce a sense of direction by detection of phase. An auxiliary unit[21] developed for use with this transformer provides an alternating-current power source of 1000 cycles, a sense-discriminating circuit, and rectifier such that direct-current rather than alternating-current output is obtained from the unit which is proportional to motion of the core, with a sense of direction.

Inasmuch as the sensitivity of the differential-transformer unit is influenced by local magnetic disturbances and by the length of electrical cable, calibration could be performed only after attachment to the ring. As shown in Figure 29, this calibration was accomplished by means of a brass screw which engaged the core and which could be advanced through a controlled displacement by means of a thumb nut. This displacement was accurately measured with a dial indicator, and calibration was performed in increments of

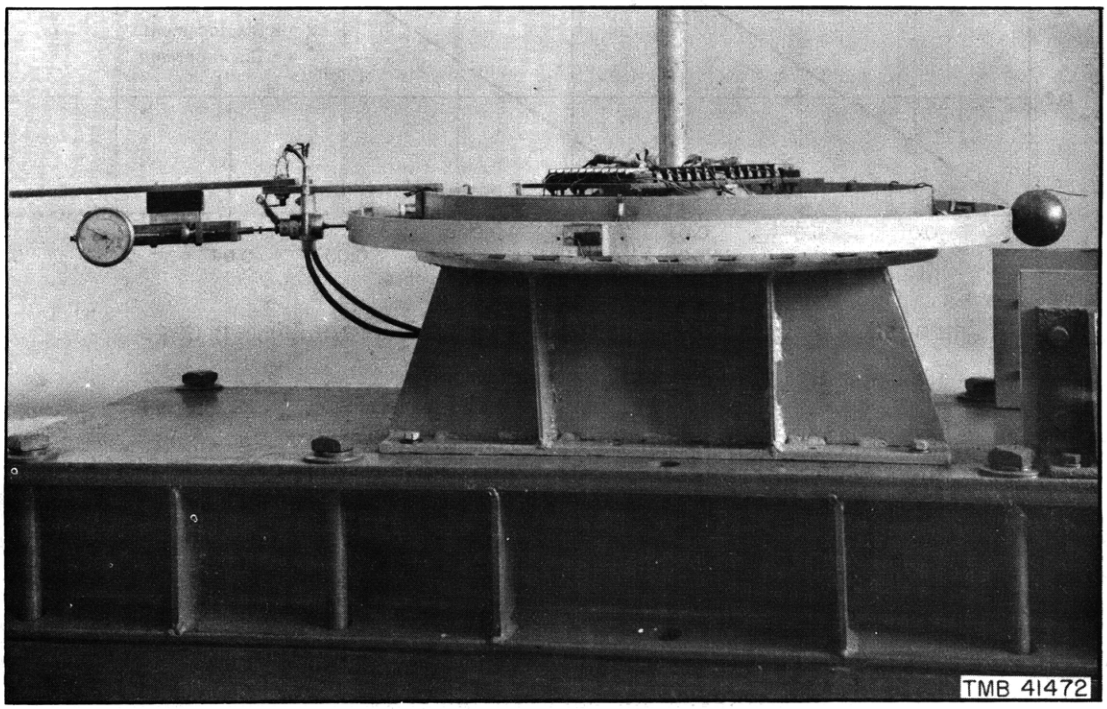

Figure 29 - Calibration of Displacement Gages

The calibration was performed by means of a brass screw, attached to the moveable transformer core, which could be advanced through a desired displacement by means of a thumb nut. This displacement was accurately measured with a precision dial indicator. Calibration was performed in increments of 0.01 in. up to a maximum displacement of 0.05 in., both inward and outward.

0.01 in. up to 0.05 in., both away from and toward the center of the ring. The Model 18-L transformer employed in the test has a range of 1/16-0-1/16 in.

A typical calibration is shown in Figure 30. Contrary to claims of the manufacturer, the calibrations were found to be somewhat erratic and nonlinear, but within the range employed the instruments were probably reliable to within 10 percent.

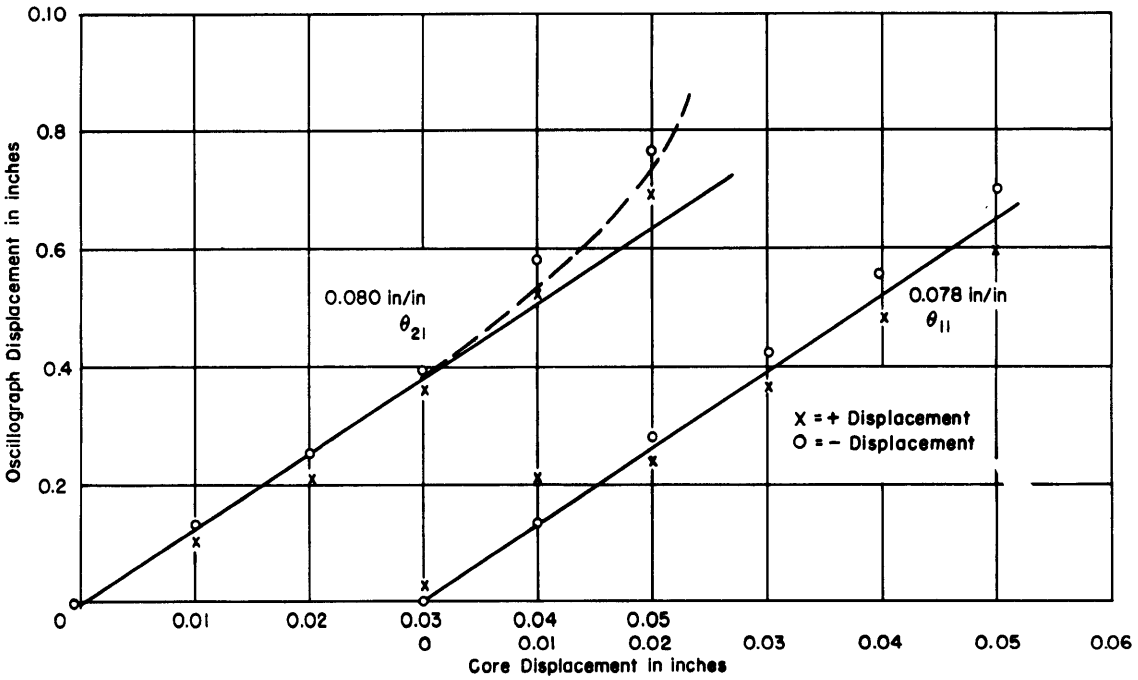

Figure 30 - Calibration of Differential Transformer Gage

H. AUXILIARY AMPLIFYING AND RECORDING EQUIPMENT

For this test where, because of the choice of ring geometry and modulus of elastic support, the important frequencies of vibration were expected to be less than 300 cps, the TMB Type 1A strain indicator was selected as an auxiliary component of the strain gage circuit.[19] This unit comprises a combination source of alternating-current power or carrier for the strain gages, an amplifier, and a demodulating or rectifying element which produces a d-c output sufficient to drive a galvanometer in a string oscillograph. The unit also incorporates calibration and attenuating circuits.

These strain indicators are designed to drive galvanometers which have a sensitivity of 4 ma/in. with an impedance of approximately 12 ohms. Response is exactly linear from 0 to 120 cycles, with a drop in response of

approximately 10 percent at 200 cycles. These units are designed to operate from two 120-ohm strain gages electrically connected to form the two external arms of a Wheatstone bridge, and the calibration system is based on a strain-gage resistance of exactly 120 ohms with a gage factor of 2.00. Any departure from these two strain-gage properties requires a correction of the calibration factors marked on the indicator.

Calibration of the strain-gage circuits is achieved by introducing into the one arm of the bridge a change in resistance which corresponds to a pre-ordained strain. To minimize the effects of contact resistance which otherwise might render inaccurate the value of the calibration constant, there is connected in series with each of the two external strain gages a 2-ohm resistance which may be then shunted as desired with a fixed precision resistor.

Because these amplifiers are sensitive to changes in both resistance and capacitance, provision is made for both capacitance and resistance balance. Ordinarily the capacitance of a circuit, once balanced, remains constant throughout the test,* but this may not be achieved if the electrical leads of the circuit are in any way disturbed. Consequently, precautions were taken to bond all electrical leads firmly so that they would not vibrate.

The displacement gages were connected as previously described to a driver and demodulator unit, Type 10-L.[21] This unit furnished 1000-cycle alternating current to power the transformers and also served as a sense discriminator and rectifier to produce d-c output. When the Type 18-L transformers were used, the output from the driving unit was about 1 mil for maximum deflection of the ring.

From the point of view of both economy in time and ease of comparison between the time history of load and the response to such excitation, it was desired to record simultaneously the electrical output of as many different gages as possible. The most suitable registering instrument for this purpose is a recording oscillograph which sometimes contains in one unit as many as 36 recording channels.

These oscillographs make use of electrical galvanometers for registering the electrical output of measuring instruments. Recording is accomplished on photographic film or sensitized paper which is driven at a selected speed past an optical slit through which the image of the light source reflected from each galvanometer element is viewed. Although the driving

---

*It is also important that the change in resistance imposed on the system during the calibration procedure not be accompanied by any change in capacitance. At the beginning of the test, a spurious calibration indication was observed due to some extraneous capacitance effect associated with operation of the switch, but this effect was remedied by the use of a trimmer condenser appropriately inserted in the calibration circuit.

machinery is arranged to advance the film at constant speed, it is not relied upon for establishment of the time scale and for this purpose an auxiliary system is provided to automatically place lines on the moving paper which represent equal intervals of time.

For this particular test a Consolidated Engineering string oscillograph, Type 5-101B, was employed with 14 galvanometer elements.[31] Recording was made on plastic impregnated sensitized paper, 8 in. wide, as manufactured by Grant Products Corporation.

Two types of galvanometers were employed for the test: A Type 7-120 having a sensitivity, with proper shunting resistance, of 5 mils/in. with a frequency range (flat plus or minus 5 percent) of 480 cycles, and a Type 7-114 with a sensitivity of 0.760 mil/in. and a frequency range of 225 cps. The Type 7-120 was used to record the output from the strain indicators, and the Type 7-114, with greater sensitivity, was employed with the deflection gages. The frequency response of both elements was considered adequate for the test.

Although a timing system was provided in the oscillograph to establish lines on the moving paper which represent time intervals of 1/100 sec, previous experience has indicated that malfunctioning of the electrical oscillator used to drive the timing motor could occur without detection, in which case serious errors in the time scale would be introduced. As a safeguard against this possibility there was recorded on one channel of the oscillograph a 60-cycle trace taken from the power line through a suitable dropping resistor.

A photograph of the auxiliary amplifying and recording equipment is given in Figure 11 on page 30.

I. DISCUSSION OF EXPERIMENTAL ERRORS

Generally, experimental errors are classified either as systematic or accidental. They differ in that the analyst can minimize accidental errors by repetition and by the exercise of careful techniques; whereas, with a given set of equipment, the systematic errors are irreducible. With wire-resistance gages the systematic errors occur in the gage factor of the strain gage, in the calibration resistors of auxiliary equipment and in the instruments employed to measure properties of the material on which strain may be measured. Accidental errors arise from the manual observations of properties of materials or scaling of records and from improper functioning of equipment.

In this study the strain gages were employed to indicate tha magnitude of bending moment at the section where the gages were mounted. The errors in measurement are:

	Percent
Gage factor of strain gage	2
Calibration resistor of strain indicator	1/2
Dimensions of ring section	1
Modulus of elasticity of ring	2
Scaled amplitude of response	2
Nonlinearity or drift in electronic equipment	1
Scaled amplitude of calibration step	1
Nonlinearity of galvanometer	1
Location of two strain gages on opposite sides of ring at different distances from neutral axes due to different thickness of adhesives	2
Total	12 1/2.

The displacement gages demonstrated some nonlinearity as well as some discrepancy in the sensitivity factor for displacements toward as compared with displacements away from the center of the ring. The various experimental errors believed associated with the measurement of displacement are:

	Percent
Calibration of dial gage	1/2
Scaled amplitude of calibration step	1
Scaled amplitude of record	4
Nonlinearity of gage and indicator	10
Drift in gage and indicator	3
Nonlinearity of galvanometer	1
Total	19 1/2

By a similar evaluation, the errors in load measurement are:

	Percent
Dynamometer	1/2
Calibration resistor of strain indicator	1/2
Scaled amplitude of response	2
Scaled amplitude of calibration	2
Nonlinearity of electronic equipment	1
Nonlinearity of galvanometer	1
Total	7

Maximum experimental errors in the parameters are thus approximately:

	Percent
Observed load P	7
Observed moment M	12
Observed displacement u	19
Elastic support k	5
Ring dimensions I and A	1
Ring radius r	1/4

These values for P, M, and u are the greatest possible errors that could occur in a single measurement, and it is unlikely that all such errors would occur simultaneously. Statistically, the chance of such an occurrence is greatly reduced if the tests are repeated and an average of the results is chosen. With a dynamic test, however, the point for point averaging of a number of oscillograms is very difficult and, in general, it is not practicable to average any but the maximum observed values. This comparison was made on many tests and it was found that repeated agreement between maximum values could be obtained within 5 percent for both strain and displacement measurement. It is, therefore, believed that even though the maximum errors in load, bending moment and displacement are 7, 12 1/2, and 19 1/2 percent, respectively, the systematic errors are less than one-half of these values; that is, 3, 5, and 8 percent respectively.

REFERENCES

1. Boussinesq, J., "Résistance d'un anneau à la flexion, quand sa surface extérieure supporte une pression normale, constante par unité de longuer de sa fibre moyenne," Acad. Sci., Paris, Comptes Rendus, Vol. 97, 1883, p. 843.

2. Lamb, H., "On the Flexure and Vibrations of a Curved Bar," London Math. Soc., Proc., Vol. 19, 1888, p. 365.

3. Timoshenko, S., "Strength of Materials," Second Edition, Van Nostrand, Vol. 2, 1940, p. 101, 218.

4. Pippard, A.J.S., and Francis, W.E., "On a Theoretical and Experimental Investigation of the Stresses in a Radially Spoked Wire Wheel under Loads Applied at the Rim," Phil. Mag., S. 7, Vol. 11, No. 69, 1931, pp. 233-285.

5. Donnell, L.H., Gibbons, H.B., and Shaw, E.L., "Analysis of Spoked Rings," Jour. Appl. Mech., Vol. 8, No. 2, 1941, pp. 67-73.

6. Hetenyi, M.I., "Beams on Elastic Foundations," Univ. of Mich. Press, 1946.

7. Hoppe, R., "Vibrationen eines Ringes in Seiner Ebene," Jour. fur Math. (Crelle), Vol. 73, 1871, pp. 158-170.

8. Love, A.E.H., "A Treatise on the Mathematical Theory of Elasticity," Fourth Edition, Dover Publ., 1944, pp. 451-453.

9. Waltking, F.W., "Schwingungszahlen und Schwingungsformen von Kreisbogenträgern," Ingenieur-Archiv, Vol. 5, 1934, pp. 429-449.

10. Federhofer, K., "Über die Eigenschwingungen des senkrecht zu einer Ebene schwingenden Kreisbogens," Acad. Wiss. Wien., Ber., ab IIa, Vol. 145, 1936, pp. 29-50.

11. Michell, J.H., "The Small Deformations of Curves and Surfaces with Application to the Vibrations of a Helix and Circular Rings," Mess. of Math., Vol. 19, 1890, pp. 68-82.

12. Brown, F.H., "Lateral Vibrations of Ring-Shaped Frames," Franklin Inst. Jour., Vol. 218, No. 1, 1934, pp. 41-48.

13. Carrier, G.F., "On the Vibrations of the Rotating Ring," Quart. Appl. Math., Vol. 3, No. 3, 1945, pp. 235-245.

14. Timoshenko, S., "Vibration Problems in Engineering," Second Edition, Van Nostrand, 1937, pp. 405-410.

15. Hoppmann, W.H., 2nd, "Impact of a Mass on a Damped Elastically Supported Beam," Jour. Appl. Mech., Vol. 15, No. 2, June 1948.

16. Rayleigh, J.W.S., "The Theory of Sound," Second Edition, London, MacMillan and Co., 1937.

17. Salvadori, M.G., "A Mathematical Treatment of the Generalized Hertz Impact of a Mass on a Simply Supported Beam," Part II, Research Laboratories, Dept. of Civil Eng., Columbia Univ., New York, N.Y.

18. Hertz, H., "Über die Berechnung Fester Elastischer Körper," Jour. für Math. (Crelle), Vol. 92, 1881, pp. 155-170.

19. Cook, G.W., "A Carrier-Type Strain Indicator," TMB Report 565, November 1946.

20. Schaevitz, H., "The Linear Variable Differential Transformer," SESA Proc., Vol. 4, No. 2, 1947, pp. 79-88.

21. "Differential Transformer Unit Driver and Demodulator Type 10-L," TMB Electronic Instrument Instruction Manual, March 1949.

22. Wahl, A.M., "Mechanical Springs," First Edition, Penton Publ. Co., 1944.

23. Lee, E.H., "The Impact of a Mass Striking a Beam," Jour. Appl. Mech., Vol. 7, 1940, pp. 129-138.

24. Zener, C., and Fechback, H., "A Method of Calculating Energy Losses during Impact," Jour. Appl. Mech., Vol. 6, 1939, pp. 67-70.

25. Raman, C.V., "On Some Applications of Hertz's Theory of Impact," Phys. Rev., Ser. 2, Vol. 15, 1920, pp. 277-284.

26. "Design and Construction of a Hydro-Pneumatic Machine for Rapid Load Tensile Testing," California Institute of Technology Report to Army Air Force, 21 May 1947.

27. Hansen, R.J., "Controlled Impulsive-Load Testing Machine," SESA Proc., Vol. 6, No. 2, 1948, pp. 64-67.

28. Wenk, E., Jr., "An Elastic-Tube Gage for Measuring Static and Dynamic Pressures," TMB Report 627, May 1948.

29. Dobie, W.B., and Isaac, P.C.G., "Electric Resistance Strain Gages," English Univ. Press, 1948.

30. Wildhack, W.H., "Spring-Type Transducers," National Bureau of Standards News Bulletin, Vol. 32, No. 1, October 1948.

31. "Operation and Maintenance Manual Type 5-101B Recording Oscillograph," Consolidated Eng. Corp., Pasadena, California.

BIBLIOGRAPHY

Lundquist, E.E., and Burke, W.R., "General Equations for the Stress Analysis of Rings," NACA TR. 509, 1934.

Timpe, A., "Probleme der Spannungsverteilung in ebenen Systemen einfach gelöst mit Hilfe d. Airyschen Funktion," Göttingen Diss., Leipzig, 1905, or Zeit. f. Math. u. Physik, Vol. 52, 1905.

Wieghardt, K., "Über einige wirklich durchführbare Ansätze zur Berechnung von Spannungszuständen des elastischen Kreisringes," Akad. Wiss. Wien, Ber., Vol. 124, 1915, p. 1119.

Filon, L.N.G., "The Stresses in a Circular Ring," Selected Engineering Papers published by the Institution of Civil Engineers No. 12, London, 1924.

Peterson, R.E., "Natural Frequency of Gears," ASME Trans. Vol. 52, 1930, APM-52-1.

Den Hartog, J.P., "Vibration of Frames of Electrical Machines," ASME Trans., 1927-1928, APM-50-6, APM-50-11.

Hoppmann, W.H., 2nd., "Experimental Study of the Transverse Impact of a Mass on a Column," J.H.U., Tech. Rpt. 2, Navy Contract N6 ONR-243, Task Order 8, (NR-035-215).

Mindlin, R.D., "Response of Damped Elastic Systems to Transient Disturbances," Proc. S.E.S.A., Vol. 5, No. 2, 1948.

Liepmann, J.P., "General Stress Analysis of Rings with One Axis of Symmetry," J. Aero. Sci., Vol. 7, 1940, pp. 509-512.

Biot, M., "Theory of Elastic Systems Vibrating under Transient Impulses with an Application to Earthquake Proof Building," Nat. Acad. Sci., Proc., Vol. 19, No. 2, 1933, pp. 262-268.

van den Dungen, F.H., "Cours de technique des vibrations," Revue de L'ecole Polytechnique Brussels, 1926.

Woodson, J.B., "Dynamic Response of a Simple Elastic System to Antisymmetrical Forcing Functions Characteristic of Airplanes in Unsymmetrical Landing Impact," Jour. Appl. Mech., Vol. 16, No. 3, 1949, pp. 210-316.

NAVY-DPPO PRNC WASH D C